

# Global Biogeochemical Cycles

## RESEARCH ARTICLE

10.1029/2020GB006672

### Key Points:

- We compiled ~1,900  $^{14}\text{C}$  measurements of  $\text{CO}_2$ ,  $\text{CH}_4$ , DOC, and POC from the northern permafrost region
- Old carbon release increases in thawed oxic soils ( $\text{CO}_2$ ), thermokarst lakes ( $\text{CH}_4$  and  $\text{CO}_2$ ), and headwaters with thermal erosion (DOC and POC)
- Simultaneous and year-long  $^{14}\text{C}$  analyses of  $\text{CO}_2$ ,  $\text{CH}_4$ , DOC, and POC are needed to assess the vulnerability of permafrost carbon across ecosystems

### Supporting Information:

- Supporting Information S1

### Correspondence to:

C. Estop-Aragonés,  
cristian.estop@uni-muenster.de

### Citation:


Estop-Aragonés, C., Olefeldt, D., Abbott, B. W., Chanton, J. P., Czimczik, C. I., Dean, J. F., et al. (2020). Assessing the potential for mobilization of old soil carbon after permafrost thaw: A synthesis of  $^{14}\text{C}$  measurements from the northern permafrost region. *Global Biogeochemical Cycles*, 34, e2020GB006672. <https://doi.org/10.1029/2020GB006672>

Received 18 MAY 2020

Accepted 30 AUG 2020

Accepted article online 2 SEP 2020

## Assessing the Potential for Mobilization of Old Soil Carbon After Permafrost Thaw: A Synthesis of $^{14}\text{C}$ Measurements From the Northern Permafrost Region

Cristian Estop-Aragonés<sup>1,2</sup> , David Olefeldt<sup>1</sup> , Benjamin W. Abbott<sup>3</sup> , Jeffrey P. Chanton<sup>4</sup> , Claudia I. Czimczik<sup>5</sup> , Joshua F. Dean<sup>6</sup> , Jocelyn E. Egan<sup>7</sup>, Laure Gandois<sup>8</sup> , Mark H. Garnett<sup>9</sup>, Iain P. Hartley<sup>10</sup>, Alison Hoyt<sup>11</sup> , Massimo Lupascu<sup>12</sup> , Susan M. Natali<sup>13</sup>, Jonathan A. O'Donnell<sup>14</sup> , Peter A. Raymond<sup>15</sup> , Andrew J. Tanentzap<sup>16</sup>, Suzanne E. Tank<sup>17</sup> , Edward A. G. Schuur<sup>18</sup> , Merritt Turetsky<sup>19</sup>, and Katey Walter Anthony<sup>20</sup>

<sup>1</sup>Department of Renewable Resources, University of Alberta, Edmonton, Canada, <sup>2</sup>Now at Ecohydrology and Biogeochemistry Group, Institute of Landscape Ecology, University of Münster, Münster, Germany, <sup>3</sup>Department of Plant and Wildlife Sciences, Brigham Young University, Provo, UT, USA, <sup>4</sup>Department of Earth Ocean and Atmospheric Science, Florida State University, Tallahassee, FL, USA, <sup>5</sup>Department of Earth System Science, University of California, Irvine, CA, USA, <sup>6</sup>School of Environmental Sciences, University of Liverpool, Liverpool, UK, <sup>7</sup>Department of Earth Sciences, Dalhousie University, Halifax, Canada, <sup>8</sup>Laboratoire Ecologie Fonctionnelle et Environnement, Université de Toulouse, CNRS, Toulouse, France, <sup>9</sup>NEIF Radiocarbon Laboratory, Scottish Enterprise Technology Park, Rankine Avenue, East Kilbride, UK, <sup>10</sup>Geography, College of Life and Environmental Sciences, University of Exeter, Exeter, UK, <sup>11</sup>Max Planck Institute for Biogeochemistry, Jena, Germany, <sup>12</sup>Department of Geography, National University of Singapore, Singapore, Singapore, <sup>13</sup>Woodwell Climate Research Center, Falmouth, MA, USA, <sup>14</sup>National Park Service, Arctic Network, Anchorage, AK, USA, <sup>15</sup>Yale School of Forestry and Environmental Studies, New Haven, CT, USA, <sup>16</sup>Ecosystems and Global Change Group, Department of Plant Sciences, University of Cambridge, Cambridge, UK, <sup>17</sup>Department of Biological Sciences, University of Alberta, Edmonton, Canada, <sup>18</sup>Department of Biological Sciences, Northern Arizona University, Flagstaff, AZ, USA, <sup>19</sup>Department of Integrative Biology, University of Guelph, Guelph, Canada, <sup>20</sup>Water and Environmental Research Center, University of Alaska Fairbanks, Fairbanks, AK, USA

**Abstract** The magnitude of future emissions of greenhouse gases from the northern permafrost region depends crucially on the mineralization of soil organic carbon (SOC) that has accumulated over millennia in these perennially frozen soils. Many recent studies have used radiocarbon ( $^{14}\text{C}$ ) to quantify the release of this “old” SOC as  $\text{CO}_2$  or  $\text{CH}_4$  to the atmosphere or as dissolved and particulate organic carbon (DOC and POC) to surface waters. We compiled ~1,900  $^{14}\text{C}$  measurements from 51 sites in the northern permafrost region to assess the vulnerability of thawing SOC in tundra, forest, peatland, lake, and river ecosystems. We found that growing season soil  $^{14}\text{C}$ - $\text{CO}_2$  emissions generally had a modern (post-1950s) signature, but that well-drained, oxic soils had increased  $\text{CO}_2$  emissions derived from older sources following recent thaw. The age of  $\text{CO}_2$  and  $\text{CH}_4$  emitted from lakes depended primarily on the age and quantity of SOC in sediments and on the mode of emission, and indicated substantial losses of previously frozen SOC from actively expanding thermokarst lakes. Increased fluvial export of aged DOC and POC occurred from sites where permafrost thaw caused soil thermal erosion. There was limited evidence supporting release of previously frozen SOC as  $\text{CO}_2$ ,  $\text{CH}_4$ , and DOC from thawing peatlands with anoxic soils. This synthesis thus suggests widespread but not universal release of permafrost SOC following thaw. We show that different definitions of “old” sources among studies hamper the comparison of vulnerability of permafrost SOC across ecosystems and disturbances. We also highlight opportunities for future  $^{14}\text{C}$  studies in the permafrost region.

## 1. Introduction

Permafrost soils in the northern circumpolar region store 1,460 to 1,600 Pg of soil organic carbon (SOC), a globally significant amount that has accumulated over millennia (Schuur et al., 2018). Amplified warming at high latitudes is currently causing widespread thawing of permafrost, which exposes deep SOC stores to contemporary hydrological and microbial processes (Abbott et al., 2015; Huang et al., 2017; Nitze et al., 2018). The transformation and release of previously frozen SOC into the atmosphere as the

©2020 The Authors.

This is an open access article under the terms of the Creative Commons Attribution-NonCommercial License, which permits use, distribution and reproduction in any medium, provided the original work is properly cited and is not used for commercial purposes.

greenhouse gases, carbon dioxide (CO<sub>2</sub>) and methane (CH<sub>4</sub>), represent a net addition into the contemporary C cycle and further exacerbate climate change. Permafrost thaw influences surface and subsurface landscape hydrology and may mobilize previously frozen SOC into aquatic ecosystems via dissolved organic carbon (DOC) and particulate organic carbon (POC) (Abbott et al., 2014; Kokelj et al., 2005, 2013; Vonk et al., 2015) which could be further transformed into CO<sub>2</sub> and CH<sub>4</sub> (Dean et al., 2020). This permafrost C-climate feedback has been identified as one of the potentially largest feedbacks to anthropogenic climate change (Ciais et al., 2013; Koven et al., 2011), yet the magnitude and timing of this feedback is poorly constrained due to uncertainties in the form of C release and the stability of deep SOC following different modes of thaw (Harden et al., 2012; Lawrence et al., 2015; Schaefer et al., 2014; Schuur et al., 2015).

The <sup>14</sup>C content of SOC reflects the time since atmospheric CO<sub>2</sub> was fixed by vegetation and subsequently transferred to soil as organic matter, and this <sup>14</sup>C value is thus imprinted in CO<sub>2</sub>, CH<sub>4</sub>, DOC, and POC derived from that soil. Given a half-life of 5,730 years, <sup>14</sup>C can be used to assess the mean age of SOC and its derivatives of up to ~50,000 years (Schuur et al., 2016). Fluxes of CO<sub>2</sub>, CH<sub>4</sub>, DOC, and POC represent a mix of C derived from several sources of variable age such as plants and roots (years to decades), SOC (mixture of carbon of different ages in itself and varying from decades to several millennia depending on soil depth and ecosystem), or even <sup>14</sup>C-depleted geological sources (beyond 50,000 years). The relative contribution of these sources to the C flux can be estimated using <sup>14</sup>C, alone or in concert with other tracers (Abbott et al., 2016; Czimczik et al., 2006; Schuur & Trumbore, 2006; Trumbore, 2000). Over the last two decades, <sup>14</sup>C has become an increasingly common tool for assessing contributions of thawing SOC to different types of C fluxes (Trumbore, 2009). While <sup>14</sup>C is a valuable tool, it can be challenging to detect the contribution of older (depleted in <sup>14</sup>C) SOC sources at depth in ecosystem C fluxes. In particular, C fixed in the last 60 years has a significantly enriched <sup>14</sup>C signature due to aboveground nuclear weapon's testing (i.e., "bomb <sup>14</sup>C"), and CO<sub>2</sub>, CH<sub>4</sub>, DOC, and POC derived from these recent C sources can act to conceal even substantial contributions to ecosystem C fluxes from older SOC that is depleted in <sup>14</sup>C. While studies commonly apply approaches to account for this mixing of contemporary (i.e., post-1950s) and older C sources, methodologies and assumptions are generally specific to each study (e.g., Dean et al., 2018; Estop-Aragonés, Czimczik, et al., 2018; Raymond et al., 2007; Schuur et al., 2009).

The vulnerability of thawed SOC to mineralization or downstream transport may depend on the mode of permafrost degradation, and the environmental conditions that prevail following thaw (Grosse et al., 2011; Jorgenson & Osterkamp, 2005). In particular, it is likely that there will be differences for SOC thawed through active layer deepening compared to thermokarst. Deepening of the seasonally thawed active layer generally occurs gradually in response to climate warming (Brown & Romanovsky, 2008; Camill, 2005), but can be more rapid in response to disturbances such as wildfire (Burn, 1998; Fisher et al., 2016; Gibson et al., 2018; O'Donnell et al., 2011) or changes in snow cover (Jafarov et al., 2018). Alternatively, thermokarst refers to a mode of permafrost degradation where land surface collapse or downslope mass movement is caused by melting of excess ground ice (Kokelj & Jorgenson, 2013). Thermokarst often affects the whole soil profile, which may then become either completely or partially inundated along edges of expanding thermokarst lakes and peatlands, or transported downstream within fluvial networks from development of thermal erosion gullies and thaw slumps along streams and rivers (Kokelj & Jorgenson, 2013). Soil thermal erosion occurs when water melts ground ice and mechanically erodes the sediments. Thermokarst landforms are found in landscapes that cover 20% of the northern permafrost region, but which contain 50% of the region's SOC (Olefeldt et al., 2016). Thus, whether permafrost is degraded gradually by active layer deepening or by thermokarst processes will influence both the quantity of thawed SOC and the environmental conditions to which it is exposed, and thus, potentially the rate and form of permafrost SOC release (Schädel et al., 2016).

Microbial mineralization of thawed SOC and its subsequent release as CO<sub>2</sub> and CH<sub>4</sub> to the atmosphere depends on soil/sediment characteristics such as depth profiles of SOC content, origin, and diagenetic state, as well as environmental conditions such as active layer thickness, temperature, and redox state (Dutta et al., 2006; Elder et al., 2018; Estop-Aragonés, Czimczik, et al., 2018; Hicks Pries et al., 2013; Lupascu et al., 2014; Vonk et al., 2013). Together, these factors influence the quantity and quality of SOC that can be thawed at a given location and determine the environmental conditions and the activity of microbial communities after thaw (Jansson & Taş, 2014; Mackelprang et al., 2016). Anoxic conditions that are prevalent in



lowland environments such as peatlands and in lakes generally have slower overall microbial activity, but increased potential for  $\text{CH}_4$  production (Cooper et al., 2017; Klapstein et al., 2014; Nakagawa et al., 2002; Walter et al., 2008). Downstream transport of DOC and POC derived from thawed SOC depend on the hydrological connectivity and flow paths between soils and fluvial networks, in-stream processing of C, and on the susceptibility of near-stream soils and river banks to erosion (Barnes et al., 2018; Mann et al., 2015; McClelland et al., 2016; Raymond et al., 2007). Laterally transported DOC and POC may be stored long term in aquatic and oceanic sediments, but may also be mineralized during transport, contributing to  $\text{CO}_2$  and  $\text{CH}_4$  emissions from peatlands, rivers, lakes, and the Arctic Ocean (Letscher et al., 2011; Regnier et al., 2013; Spencer et al., 2015; Tank et al., 2018).

Here we compile and review information from all currently available studies carried out in the northern permafrost region where C fluxes ( $\text{CO}_2$ ,  $\text{CH}_4$ , DOC, POC) have been characterized using  $^{14}\text{C}$ . Our goals were to (1) contrast differences and variability in  $^{14}\text{C}$  signatures across ecosystems and forms of C, (2) link variability in  $^{14}\text{C}$  signatures to landscape characteristics and environmental conditions, (3) compile rates of “old” SOC release estimated among studies and compare methodologies for such estimates, and (4) assess consistency across studies of broad ecosystem classes with regards to the influence of disturbances and mode of thaw on the vulnerability of permafrost SOC. A further aim of this synthesis is to reveal challenges and opportunities for future  $^{14}\text{C}$  studies in the region since it represents one of the key methodologies for reducing the uncertainty of the permafrost C feedback to climate change.

## 2. Materials and Methods

### 2.1. Database Compilation

We compiled a database of  $^{14}\text{C}$  measurements of  $\text{CO}_2$ ,  $\text{CH}_4$ , DOC, and POC from the northern permafrost region. We defined this region based on the permafrost coverage previously outlined (Brown et al., 1997). The database included data from 50 studies, mostly published prior to May 2018, identified through Web of Science using the keywords “radiocarbon  $\text{CO}_2$  permafrost”, “radiocarbon  $\text{CH}_4$  permafrost”, “radiocarbon DOC permafrost”, or “radiocarbon POC permafrost”. Additional studies were identified through citations in the reviewed studies (Table 1). We focused on  $^{14}\text{C}$  measurements of gaseous soil emissions and waterborne ecosystem C fluxes but the database also included C forms belowground, such as soil gases and pore water DOC. We did not include  $^{14}\text{C}$  measurements of the SOC pool, which can provide estimates of SOC turnover at decadal to millennial time-scales (e.g., He et al., 2016) but provide little information on the form of C release to the atmosphere or aquatic ecosystems. Further, we did not include compound-specific  $^{14}\text{C}$  analysis, such as plant wax lipid compounds, lignin phenols, or hydroxy phenols. Most of the  $^{14}\text{C}$  data were obtained from tables in the studies, or were provided by authors, but some data (143  $^{14}\text{C}$  measurements) were approximated from figures if no other options were available. The data set (DOI 10.5281/zenodo.3832031) is available at <https://zenodo.org/record/3832031#.XsJ8vntCSUI> and has also been included in the ISRaD repository (<http://www.soilradiocarbon.org>).

We classified  $^{14}\text{C}$  measurements to be associated with five broad ecosystem types: tundra, boreal forest, peatlands, lakes, and rivers/streams. Ecosystem classification was based on descriptions provided in the published studies. Further, many studies used natural or experimental disturbances to assess vulnerability of thawed SOC, and we classified  $^{14}\text{C}$  data to be associated with either undisturbed or disturbed sites within each ecosystem type. We considered disturbed sites to include active layer thaw gradients (tundra), warming/wetting/drying manipulations (tundra and one peatland), wildfire (tundra and boreal forest), and thermokarst (lakes, peatlands, and streams). Data were further grouped by C form ( $\text{CO}_2$ ,  $\text{CH}_4$ , DOC, and POC) in order to assess the effects of disturbance on  $^{14}\text{C}$  of  $\text{CO}_2$  and  $\text{CH}_4$  and highlight the  $^{14}\text{C}$  variability of DOC and POC along the soil-stream-river continuum (supporting information Table S1).

We grouped gaseous ( $\text{CO}_2$ ,  $\text{CH}_4$ ) measurements by collection method, distinguishing samples released to the atmosphere and those obtained belowground. Measurements released to the atmosphere included soil chamber gas emissions, bubbles, and dissolved gas from surface waters. Belowground gaseous measurements included incubations and soil gas samples collected in situ in the pore space with probes. We categorized DOC and POC data into soil pore water versus tributaries or main stem of major rivers in order to

**Table 1**  
List of Studies Measuring  $^{14}\text{C}$  of  $\text{CO}_2$ ,  $\text{CH}_4$ ,  $\text{DOC}$ , and  $\text{POC}$  in the Northern Permafrost Region

ID	Reference	$^{14}\text{C}$ dating	Location	Study and ecosystem description
1	Czimczik and Welker (2010)	$\text{CO}_2$	Greenland	Flux in High Arctic tundra (soil pore space, incubations)
2	Lupascu, Welker, Seibt, et al. (2014)	$\text{CO}_2$	Greenland	Flux in High Arctic tundra (manipulation, soil pore space, incubations)
3	Lupascu et al. (2014)	$\text{CO}_2$	Greenland	Flux in High Arctic tundra (manipulation, soil pore space, incubations)
4	Schuur et al. (2009)	$\text{CO}_2$	Interior Alaska (AK)	Flux in tundra thaw gradient (soil pore space, incubations)
5	Hicks Pries et al. (2013)	$\text{CO}_2$	Interior AK	Flux in tundra thaw gradient (incubations)
6	Natali et al. (2015)	$\text{CO}_2$	Interior AK	Flux in tundra thaw gradient (manipulation, soil pore space)
7	Natali et al. (2011)	$\text{CO}_2$	Interior AK	Flux in tundra thaw gradient (manipulation, soil pore space)
8	Hicks Pries et al. (2016)	$\text{CO}_2$	Interior AK	Flux in tundra thaw gradient (manipulation, incubations)
9	Hicks Pries et al. (2015)	$\text{CO}_2$	Interior AK and Sweden	Flux in tundra and in subarctic bog (manipulation, incubations)
10	Lee et al. (2012)	$\text{CO}_2$	Interior and N Slope AK	Incubations of tundra soils and soil fractions
11	Nowinski et al. (2010)	$\text{CO}_2$	N Slope AK	Flux in tundra (manipulation, soil pore space, incubations)
12	Klapstein et al. (2014)	$\text{CO}_2$ , $\text{CH}_4$	Interior AK	Ebullition in thermokarst bog
13	Cooper et al. (2017); Estop-Aragonés, Cooper, et al. (2018)	$\text{CO}_2$ , $\text{CH}_4$	W Canada	Flux in peat plateaus, thermokarst bogs, burnt, and intact forests in Yukon and Northwest Territories (NT) (soil pore space)
14	Estop-Aragonés, Czimczik, et al. (2018)	$\text{CO}_2$	W Canada: Northern Alberta	Flux in peat plateaus, burnt peat plateaus, and thermokarst bogs (soil pore space)
15	Gandois et al. (2019) and novel data	$\text{CO}_2$ , $\text{CH}_4$ , $\text{DOC}$	W Siberia	Ebullition and waters in peat palsa and thermokarst lake
16	Dutta et al. (2006)	$\text{CO}_2$ , $\text{DOC}$	E Siberia	Yedoma soils in Kolyma lowlands
17	Dean et al. (2018)	$\text{CO}_2$ , $\text{CH}_4$ , $\text{DOC}$	W Canada: Northwest Territories (NT)	Dissolved gas and waters in polygonal ponds, streams, and lakes
18	Novel data	$\text{CO}_2$	E Siberia and AK	Flux in boreal forest, burnt, and intact tundra
19	Martens et al. (1992)	$\text{CH}_4$	AK	Ebullition in tundra lakes in Yukon-Kuskokwim
20	Zimov et al. (1997)	$\text{CH}_4$	E Siberia	Ebullition in thermokarst lakes
21	Nakagawa et al. (2002)	$\text{CH}_4$	E Siberia	Ebullition in thermokarst lakes
22	Walter Anthony et al. (2016)	$\text{CH}_4$	E Siberia, Sweden, and AK	Ebullition in thermokarst lakes
23	Walter et al. (2008)	$\text{CO}_2$ , $\text{CH}_4$	E Siberia and Interior AK	Ebullition in lakes and thermokarst lakes
24	Bouchard et al. (2015)	$\text{CO}_2$ , $\text{CH}_4$	E Canada: Nunavut	Ebullition in lakes and thermokarst lakes in Bylot Island
25	Negandhi et al. (2013)	$\text{CO}_2$ , $\text{CH}_4$	E Canada: Nunavut	Ebullition in lakes and thermokarst lakes in Bylot Island
26	Elder et al. (2018)	$\text{CO}_2$ , $\text{CH}_4$	N Slope, AK	Dissolved gas in thermokarst lakes
27	Raymond et al. (2007)	$\text{DOC}$	E Siberia, W Siberia, W Canada, and AK	Main stem of Arctic Great Rivers: Yenisey, Lena, Ob', Mackenzie, and Yukon
28	Amon et al. (2012)	$\text{DOC}$	E Siberia, W Siberia, W Canada, and AK	Main stem of Arctic Great Rivers: Kolyma, Yenisey, Lena, Ob', Mackenzie, and Yukon
29	McClelland et al. (2016)	$\text{POC}$	E Siberia, W Siberia, W Canada, and AK	Main stem of Arctic Great Rivers: Kolyma, Yenisey, Lena, Ob', Mackenzie, and Yukon
30	Holmes et al. (2018)	$\text{DOC}$ , $\text{POC}$	E Siberia, W Siberia, W Canada, and AK	Main stem of Arctic Great Rivers: Kolyma, Yenisey, Lena, Ob', Mackenzie, and Yukon
31	Striegl et al. (2007)	$\text{DOC}$	AK	Main stem and large tributaries of Yukon river
32	O'Donnell et al. (2014)	$\text{DOC}$ (HPOA)	AK	Large tributaries of Yukon river; HPOA = hydrophobic organic acid fraction of dissolved organic matter
33	Aiken et al. (2014)	$\text{DOC}$	W Canada and AK	Main stem, tributaries, and glacial waters of Yukon river
34	Guo and Macdonald (2006)	$\text{DOC}$ , $\text{POC}$	AK	Main stem of Yukon river
35	Guo et al. (2003)	$\text{DOC}$ , $\text{POC}$	AK	Main stem of Chena river
36	Ewing et al. (2015)	$\text{DOC}$	AK	Yedoma SOC leachates from yedoma near Hess Creek
37	Drake et al. (2015)	$\text{DOC}$	AK	Yedoma SOC leachates in Fox permafrost tunnel
38	Guo et al. (2007)	$\text{DOC}$ , $\text{POC}$	W Canada and AK	Main stem and SOC leachates from Mackenzie, Sagavanirktok, and Yukon rivers
39	Neff et al. (2006)	$\text{DOC}$	E Siberia	Main stem and tributaries of Kolyma river
40	Mann et al. (2015)	$\text{DOC}$	E Siberia	Main stem, tributaries, and yedoma leachates of Kolyma river
41	Vonk et al. (2013)	$\text{DOC}$ , $\text{POC}$	E Siberia	Yedoma riverbank collapse thaw streams of Kolyma river
42	Hilton et al. (2015)	$\text{POC}$	W Canada	Main stem and large tributaries of Mackenzie river
43	Littlefair et al. (2017)	$\text{DOC}$	W Canada	Retrogressive thaw slumps (thaw streams) in Peel Plateau, NT
44	Hood et al. (2009)	$\text{DOC}$	AK	Glaciated and unglaciated watersheds in Gulf of Alaska



**Table 1**  
*Continued*

ID	Reference	<sup>14</sup> C dating	Location	Study and ecosystem description
45	Stubbins et al. (2012)	DOC	AK	Glacial water in Mendenhall and Gulkana Glaciers
46	Benner et al. (2004)	DOC	W Siberia and N Slope AK	Main stem of Kokolik and Ikpiqruk rivers and Yenisey and Ob' rivers
47	Amon and Meon (2004)	DOC	E Canada	Main stem of Hudson Bay rivers
48	Godin (2014)	DOC, POC	E Canada: Nunavut	Lake and streams in Frobisher Bay, Baffin Island
49	Abbott and Stafford (1996)	DOC	W Canada: Northwest Territories (NT)	Peat pore water and streams in burnt and intact watersheds
50	Burd et al. (2018) and novel data	DOC		

characterize different sources and account for  $^{14}\text{C}$  variability along the soil-stream-river continuum. DOC was defined as organic C passing through a 0.2- to 1- $\mu\text{m}$  filter (generally 0.45  $\mu\text{m}$ ) depending on the study, whereas POC reflects the size class of organic C that cannot pass through the filter. Soil pore water included in situ sampling in thaw streams (thaw slump rill water), and waters obtained in the laboratory from soil cores and soil leachates. Samples from tributaries were collected from small and large streams as defined by the studies and were classified as either glaciated or unglaciated catchments. We refer to glaciated catchments for data collected in tributaries draining present-day glaciers. For clarity, the few available DOC and POC data from lakes (26  $^{14}\text{C}$  measurements) were considered to be part of the catchment drainage network and, thus, were merged into the nonglaciated tributary category. Many of the compiled DOC and POC data came from the sampling of mainstem locations on the six largest Arctic rivers by the Arctic Great Rivers Observatory (ArcticGRO; <https://arcticgreatrivers.org/>) (e.g., McClelland et al., 2016; Raymond et al., 2007). For all sites,  $\delta^{13}\text{C}$  (Figure S1) and other ancillary data were compiled when available (sampling date, coordinates, discharge, concentrations).

Data were also grouped by region to characterize the spatial distribution of measurements across the circumpolar North; including Alaska, Western Canada, Eastern Canada, Greenland, Europe, Western Siberia, and Eastern Siberia (Figure 1). Western Canada included data from Yukon, Northwest Territories (NT), and Alberta. Eastern Canada included data from Nunavut and the Hudson Bay Lowlands. Europe refers uniquely to data from Sweden. We used the catchment area of the Yenisey River to differentiate between Western and Eastern Siberia. Data on  $^{14}\text{C}$  of DOC and POC from the main stems of ArcticGRO rivers are included in these regions as follows: Alaska (Yukon River), Western Canada (Mackenzie River), Western Siberia (Ob' and Yenisey Rivers), Eastern Siberia (Lena and Kolyma Rivers).

All  $^{14}\text{C}$  data were converted to fraction modern ( $fM$ ) using defined equations (Stuiver & Polach, 1977):

$$\Delta^{14}\text{C} \left( \text{‰} \right) \text{ to } fM \quad fM = \frac{\frac{\Delta^{14}\text{C} \left( \text{‰} \right)}{1000} + 1}{e^{\lambda(1950 - Y_s)}}, \quad (1)$$

$$^{14}\text{C} \text{ age to } fM \quad fM = e^{\left( \frac{\text{Age}}{-8033} \right)}, \quad (2)$$

$$\% \text{Modern to } fM \quad fM = \frac{\% \text{Modern}}{100}, \quad (3)$$

where  $\lambda$  equals  $1/8,267 \text{ year}^{-1}$  (i.e.,  $1/\text{true mean life of radiocarbon}$ ),  $Y_s$  represents the year of sampling (we assume the  $^{14}\text{C}$  analysis was in the same year as sample collection unless stated), and Age represents the uncalibrated age ( $^{14}\text{C}$  age expressed as years before present where present is CE 1950). By convention, the  $^{14}\text{C}$  content is corrected for mass-based fractionation effects using stable C isotope ( $\delta^{13}\text{C}$ ) value of  $-25 \text{ ‰}$ , and is expressed relative to a standard representing the preindustrial atmospheric  $^{14}\text{C}\text{-CO}_2$  in 1950. As such, the age of  $^{14}\text{C}$  measurements can be expressed as years before present (years BP) where present refers to CE 1950 (0 years BP,  $fM = 1$ ), and samples with a higher  $^{14}\text{C}$  content than atmospheric  $^{14}\text{C}\text{-CO}_2$  in 1950 are referred to as modern ( $fM > 1$ ).

Our study also included data (95  $^{14}\text{C}$  measurements) from unpublished studies, which were obtained from members of the Permafrost Carbon Network (<http://www.permafrostcarbon.org>). These data included  $\text{CO}_2$  and  $\text{CH}_4$  from thermokarst peatlands in W Siberia,  $\text{CO}_2$  from tundra in Alaska and boreal forest in E Siberia, and DOC from streams draining peatlands in W Canada (Table 1). Samples from thermokarst peatlands in W Siberia were collected using either bubble traps (ebullition samples) or piezometers connected to a hand pump (porewater samples:  $\text{CO}_2$  and  $\text{CH}_4$  degassed into the headspace of 1 L glass bottle with a peristaltic pump) and the gas samples were stored in sealed 200 ml preevacuated bottles. The  $\text{CO}_2$  and  $\text{CH}_4$  were separated in a vacuum line before  $^{14}\text{C}$  analysis as previously described (Pack et al., 2015). Samples for ecosystem respiration from tundra in Alaska and boreal forest in E Siberia were collected using gas canisters connected to dark static chambers after an enclosure time of approximately 30 min and were corrected for atmospheric  $^{14}\text{C}$  content (Lupascu, Welker, Xu, et al., 2014). Water sampling for  $^{14}\text{C}\text{-DOC}$  analysis from peat porewater and streams in W Canada followed the same procedures as described in a preliminary study sampling the sites (Burd et al., 2018).



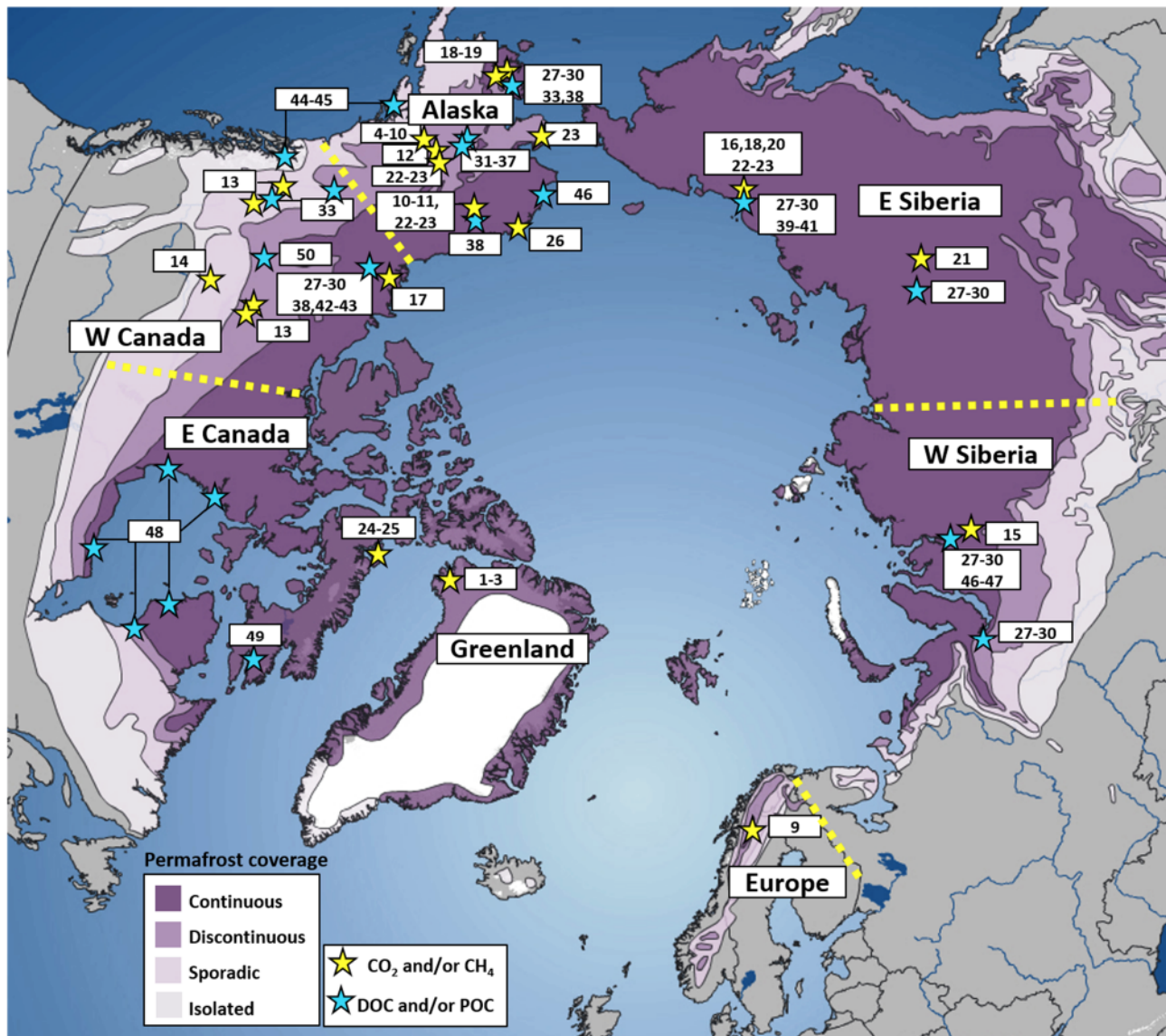


**Figure 1.** Site locations for  $^{14}\text{C}$  measurements of  $\text{CO}_2$ ,  $\text{CH}_4$ , DOC, and POC in the northern permafrost region with permafrost coverage as previously defined (Brown et al., 1997). Numbers indicate the study ID listed in Table 1. For clarity, not all specific locations associated with a measurement are included. Dashed lines separate the seven regions discussed in text: Alaska, Western Canada, Eastern Canada, Greenland, Europe, Western Siberia, and Eastern Siberia.

## 2.2. Review of Controls and Estimates of “Old” SOC Release

We present this data set by plotting the compiled  $^{14}\text{C}$  measurements across regions, ecosystems, C forms, and type of disturbance. We did not consider it appropriate to use other statistical analysis due to the unbalanced data set and the lack of other data associated to the  $^{14}\text{C}$  measurements. We related the variability in  $^{14}\text{C}$  signatures to landscape characteristics and environmental conditions by reviewing the major controls identified in the studies. The  $^{14}\text{C}$  values of  $\text{CO}_2$ ,  $\text{CH}_4$ , DOC, and POC were not linked to other continuous data such as thaw depth, soil temperature, soil moisture, productivity, SOC content, or SOC age for most studies and, thus, were not compiled for this study. Instead, we reviewed the importance of these controls on the compiled  $^{14}\text{C}$  data based on the findings from the studies. For example, relationships between  $^{14}\text{C}$  of C fluxes and  $^{14}\text{C}$  of SOC are broadly discussed as a possible driver of variability of measurements across ecosystems and regions. In this regard, given their older SOC age, we refer to “Pleistocene-aged” landscapes to group measurements in locations mostly not covered by the Eurasian, Laurentide, and Cordilleran ice sheets

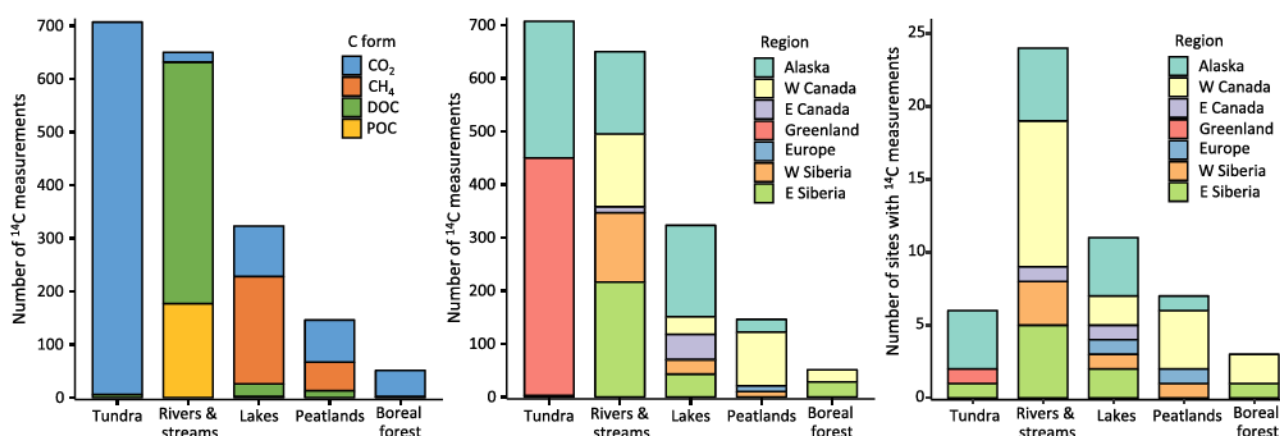


**Figure 2.** Classification of  $^{14}\text{C}$  measurements by ecosystem type among (a) C forms ( $\text{CO}_2$ ,  $\text{CH}_4$ , DOC, and POC) and (b) geographical region, and (c) number of sites among geographical regions. Counts include all  $^{14}\text{C}$  measurements (fluxes and belowground measurements).

that extended from west of the Lena River to Alaska and parts of the Yukon Territory (Grosse et al., 2013; Schirrmeister et al., 2013). Such Pleistocene-aged measurements mostly come from terrain underlain by ice-rich loess sediments in Yedoma regions but also include regions where glaciogenic tills are overlain by Holocene-age organic matter in soils (Littlefair et al., 2017).

While raw  $^{14}\text{C}$  measurements can indicate the relative contribution of “old” SOC to a C flux, it cannot by itself be used to assess the absolute rate of “old” SOC mobilization. Estimating the rate of “old” SOC release requires, at least, both  $^{14}\text{C}$  data as well as a measure of overall C flux rate. Our database does not include information about the ecosystem C fluxes associated with each  $^{14}\text{C}$  measurement, as such paired data were not provided in the majority of studies. Thus, we did not perform any new isotopic source apportionment analysis, but we provide a summary of different approaches that have been used to partition C fluxes into various C sources (or end-members) of distinct  $^{14}\text{C}$  ages and to calculate rates of “old” SOC loss. The relative contribution of C sources to a C flux was typically calculated using isotopic end-member mixing models with a simple mass-balance approach, or through probability distributions using a Bayesian approach (Moore & Semmens, 2008). One problem with comparing estimated contributions and rates of “old” SOC release is that “old” is a relative term and each study has its own definition. Our summary assessed differences in the definition of “old” C sources across studies, and showed how these definitions of “old” C sources influenced estimated rates of “old” SOC mobilization. Lastly, this summary was used to evaluate and contrast the effects of disturbances on thawed SOC mineralization across ecosystems and mode of thaw.

### 3. Results

#### 3.1. Radiocarbon Data From the Northern Permafrost Region

The compiled database included 1,877  $^{14}\text{C}$  measurements from 51 sites, of which 50% were associated with  $\text{CO}_2$ , 14% with  $\text{CH}_4$ , 27% with DOC, and 9% with POC (Figure 2a). Measurements of surface-to-atmosphere greenhouse gases fluxes were overall more common than belowground measurements, which accounted for 41% of the total  $\text{CO}_2$  data and 12% for  $\text{CH}_4$ . Similarly, most  $^{14}\text{C}$  measurements of DOC and POC were collected from streams and rivers, while belowground pore water measurements accounted for only 10% of DOC data and 3% of POC data.

The distribution of  $^{14}\text{C}$  measurements among ecosystems, regions, and C forms was not even (Figure 2). Tundra ecosystems had the most measurements at 700, compared to only 50 from the boreal forest, despite the much greater size of the boreal forest within the permafrost region. Measurements from tundra and boreal forests were both dominated by  $\text{CO}_2$  measurements, while there was a greater diversity in measured C forms for lakes and peatlands (Figure 2a). In total, 32% of the  $^{14}\text{C}$  data were from Alaska, 24% from Greenland, 16% from Western Canada, 15% from Eastern Siberia, 9% from Western Siberia, 3% from Eastern Canada, and 1% from Europe (Figure 2b). In our database, 90% of the 700  $^{14}\text{C}$  measurements from tundra ecosystems were from



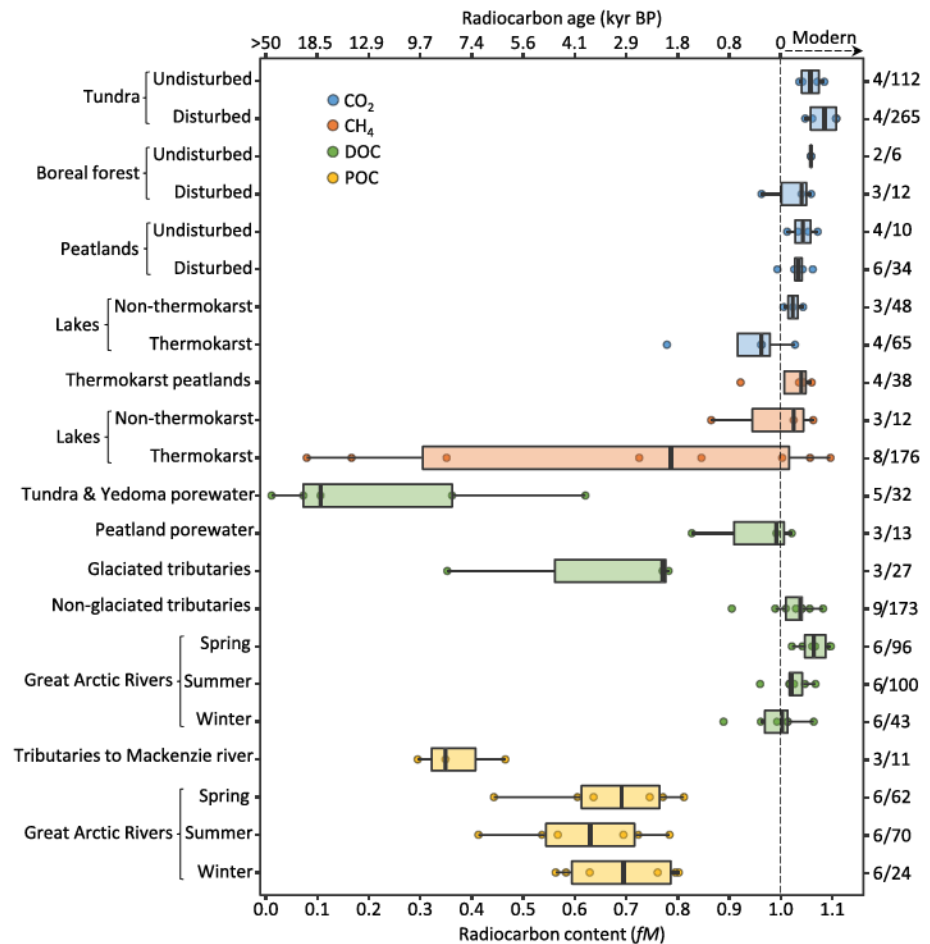


**Figure 3.** Summary of radiocarbon content of  $CO_2$ ,  $CH_4$ , DOC, and POC measured in the northern permafrost region. Data for  $CO_2$  and  $CH_4$  refers to flux measurements released to the atmosphere and excludes belowground and soil incubation measurements, whereas data for DOC and POC includes both flux and belowground measurements to highlight the soil-stream-river continuum. Disturbance includes field manipulations (warming/wetting/drying), natural or fire-induced deepening of the active layer, and thermokarst processes. Each point represents the median of  $^{14}C$  measurements from each study site (Table S1 shows the classification of sites and associated number of measurements). The boxes show the first and third quartiles, the solid vertical line is the median of medians, and the whiskers extend 1.5 times the interquartile range. On the right, the first value indicates the number of study sites and the second value indicates the total number of  $^{14}C$  measurements.

only two sites within Alaska and Greenland (Figure 2c). Data for rivers and streams were more evenly spread across regions because DOC and POC data from ArcticGRO included the largest Arctic Rivers, and the greater number of sites for this “ecosystem” category was due to sampling of high- to middle-order tributaries and smaller fluvial systems to characterize the fluvial network.

Data collected between May and September accounted for 95%, 85%, and 82% of all  $CO_2$ , DOC, and POC measurements, respectively. This distribution was more spread over the year for  $CH_4$  with 57% of measurements between May and September, due to more frequent lake measurements collected between fall and early spring.

### 3.2. Broad Patterns of C Age Across C Forms, Ecosystems, and Disturbances

We found large differences between  $^{14}C$  measurements for different C forms with regards to the proportion of reported  $^{14}C$  measurements that had modern ( $fM > 1$ ) signatures (Figure 3). This included 86% of reported  $^{14}C$ - $CO_2$  being modern, followed by 64%, 28%, and 2%, respectively, for DOC,  $CH_4$ , and POC  $^{14}C$  measurements.

Overall, 60% of all reported  $^{14}\text{C}$  measurements were modern, and included nearly all  $\text{CO}_2$  emissions from terrestrial ecosystems (tundra, boreal forest, and peatlands),  $\text{CH}_4$  emissions from peatlands, and DOC in nonglacial rivers and large Arctic rivers. Measurements in the main stem of the large Arctic rivers generally showed modern DOC, with  $^{14}\text{C}$  values decreasing from spring to winter (i.e., increasing contributions of older sources), whereas POC data were consistently premodern with no seasonal trend. The most depleted  $^{14}\text{C}$  measurements were associated with POC in large rivers, DOC in soil pore water and glacial streams, and with  $\text{CH}_4$  and  $\text{CO}_2$  emitted from lakes—particularly those associated with thawing Yedoma and Pleistocene-aged deposits.

There was not a universal trend of more  $^{14}\text{C}$  depleted C being mobilized from disturbed ecosystems where permafrost thaw had been accelerated (Figure 3). Thermokarst lakes were found to generally release more  $^{14}\text{C}$  depleted  $\text{CO}_2$  and  $\text{CH}_4$  than nonthermokarst lakes, but accelerated permafrost thaw in terrestrial ecosystems was not found to be consistently associated with more depleted  $^{14}\text{C}$ - $\text{CO}_2$  emissions than from undisturbed ecosystems (e.g.,  $\text{CO}_2$  in tundra, Figure 3). However, it is important remarking that a lack of lower  $^{14}\text{C}$  values in emissions from disturbed terrestrial sites does not preclude enhanced mineralization of more depleted SOC sources as such contributions may be obscured by concurrent increases in mineralization of modern SOC sources. For example, a greater relative contribution of more depleted SOC sources to fluxes was not associated with greater absolute rate of old SOC release if emissions of  $\text{CO}_2$  (Lupascu et al., 2018) or  $\text{CH}_4$  are low (Cooper et al., 2017). In contrast, enhancement of the autotrophic respiration component may lower the relative contribution of  $^{14}\text{C}$  depleted SOC sources to the flux but still result in greater absolute release of old SOC due to higher  $\text{CO}_2$  emissions (Hicks Pries et al., 2016). This highlights the need for information about ecosystem C fluxes and  $^{14}\text{C}$  data to determine absolute rates of “old” SOC mobilization or mineralization and evaluate the effects of disturbance.

### 3.3. Estimates of “Old” SOC Contribution and Rates of “Old” SOC Release

We documented how different studies reported relative contribution of C sources and fluxes of “old” SOC (Table S2). Nineteen studies determined the relative contribution of C sources (or end-members) to ecosystem C flux measurements. We found that the defined age of “old” SOC varied among studies from modern (see Hicks Pries et al., 2015) to a few centuries to a few millennia to >40,000 years BP (Table S2). This implies that studies using younger “old” end-members have the potential to report greater losses of “old” sources, assuming the same ecosystem C flux. The influence of such defined age on the contribution of “old” C can be presented in a mixing model with two sources (contemporary and old) to apportion a flux  $^{14}\text{C}$  measurement, with a modern  $fM$  value of 1.04. In a theoretical case, using an old SOC source aged either 500, 5,000, or 50,000 years BP and a contemporary C source reflected by the integrated annual average of atmospheric  $^{14}\text{C}$ - $\text{CO}_2$  during 1950–2012 ( $fM = 1.221$ ; Elder et al., 2018; Hua et al., 2013), the contribution of the “old” end-member represents 64%, 26%, or 15%, respectively.

Most studies used isotopic end-member mixing models to determine the relative contribution of C sources (or end-members) to ecosystem C flux measurements. The number of end-members varied from two to five and could include roots, aboveground vegetation, surface, and deeper SOC depending on the experimental design and ecosystem properties. The  $^{14}\text{C}$  (and  $\delta^{13}\text{C}$ ) values of the end-members were measured directly or prescribed from literature values. For example, incubations of aboveground and belowground plant tissues showed that  $\text{CO}_2$  respired from autotrophic sources is close to (typically above) the atmospheric  $^{14}\text{C}$ - $\text{CO}_2$  content (Figure S2). Similarly, the age of  $\text{CO}_2$  from heterotrophic respiration increased with soil depth (except for bomb  $^{14}\text{C}$  peak layers) and was used to determine the  $^{14}\text{C}$  signature of “old” SOC, as shown from incubations and in situ measurements at depth (Figure S3).

Fifteen studies reported estimates of fluxes of “old” SOC (Table S2). Most of these estimates were associated with two tundra sites, three thermokarst peatland sites, and several thermokarst lakes, while there was a single estimate for boreal forest and no reported rates of “old” SOC release across the soil-stream-river continuum. We selected specific studies to contrast the effects of disturbances on thawed SOC mineralization across broad ecosystem classes and mode of thaw (Table 2). This information will be referred to for each C form in the next sections with regards to the effects of thaw on “old” SOC vulnerability across ecosystems and type of disturbance.



**Table 2**  
*Summary of Estimates of “Old” C Release in the Northern Permafrost Region Across Ecosystems as Defined by the Studies*

Ecosystem (study ID)	Disturbance factor	Age of “old” C (years BP)	Rate of “old” C release as defined by the study <sup>a</sup>
High Arctic tundra in Greenland (2)	Soil temperature and moisture	310 to 463	Summer estimates—CO <sub>2</sub> : $7.1 \pm 2.4$ (2010), $40.5 \pm 7.8$ (2011, warm and dry year), and $23.8 \pm 6.4$ g C m <sup>-2</sup> (2012, warm and wet year)
Tundra in interior Alaska (5)	Active layer deepening	150 to 190	Growing season estimates—CO <sub>2</sub> : 30, 45, and 60 g C m <sup>-2</sup> in areas of minimal, moderate, and extensive thaw, respectively
Boreal forest and peatland in W Canada (13, 14)	Fire-induced active layer deepening	1,200	Growing season estimates—CO <sub>2</sub> : 5 to 9 and 30 g C m <sup>-2</sup> in the unburnt and burnt forest, respectively
Peatland in W Canada (13)	Thermokarst	1,200	Growing season estimates—CO <sub>2</sub> & CH <sub>4</sub> : $0.4$ g C-CO <sub>2</sub> m <sup>-2</sup> and $<1.5$ g C-CH <sub>4</sub> m <sup>-2</sup> in thermokarst peatlands versus $4$ to $9$ g C-CO <sub>2</sub> m <sup>-2</sup> in undisturbed peat plateaus
Lakes in NE Siberia (20)	Thermokarst	20,000 to 40,000	Ebullition estimate—CH <sub>4</sub> : $6.8$ to $10$ mg CH <sub>4</sub> m <sup>-2</sup> day <sup>-1</sup> in winter (April), and $0.5$ to $0.9$ mg CH <sub>4</sub> m <sup>-2</sup> day <sup>-1</sup> in summer (July)
Lakes in N Slope Alaska (26)	Thermokarst	>11,500	Diffusion estimate (annual) <sup>b</sup> —CO <sub>2</sub> and CH <sub>4</sub> : $78.60$ mg C-CO <sub>2</sub> m <sup>-2</sup> day <sup>-1</sup> and $0.65$ mg C-CH <sub>4</sub> m <sup>-2</sup> day <sup>-1</sup>
Kolyma River network (40)	Thermokarst	22,540	Rates not reported. “Old” C contribution in DOC samples August–October: 97% in yedoma thaw waters, 43% in erosion streams, 13% in streams, 6% in minor tributaries, and <1% in major tributaries and main stem

*Note.* Study numbers shown here refer to citations (ID) in Table 1. See Table S2 for a more detailed compilation of all estimates and methodologies.  
<sup>a</sup>Approximate values based on flux and estimated contribution of old C reported by the study. <sup>b</sup>Rates based on mean diffusive fluxes and flux-weighted mean contribution for the study region in N Slope AK. Winter measurements were assumed by the study to also account for ebullition due to dissolution of gases from bubbles into the water under the lake ice cover.

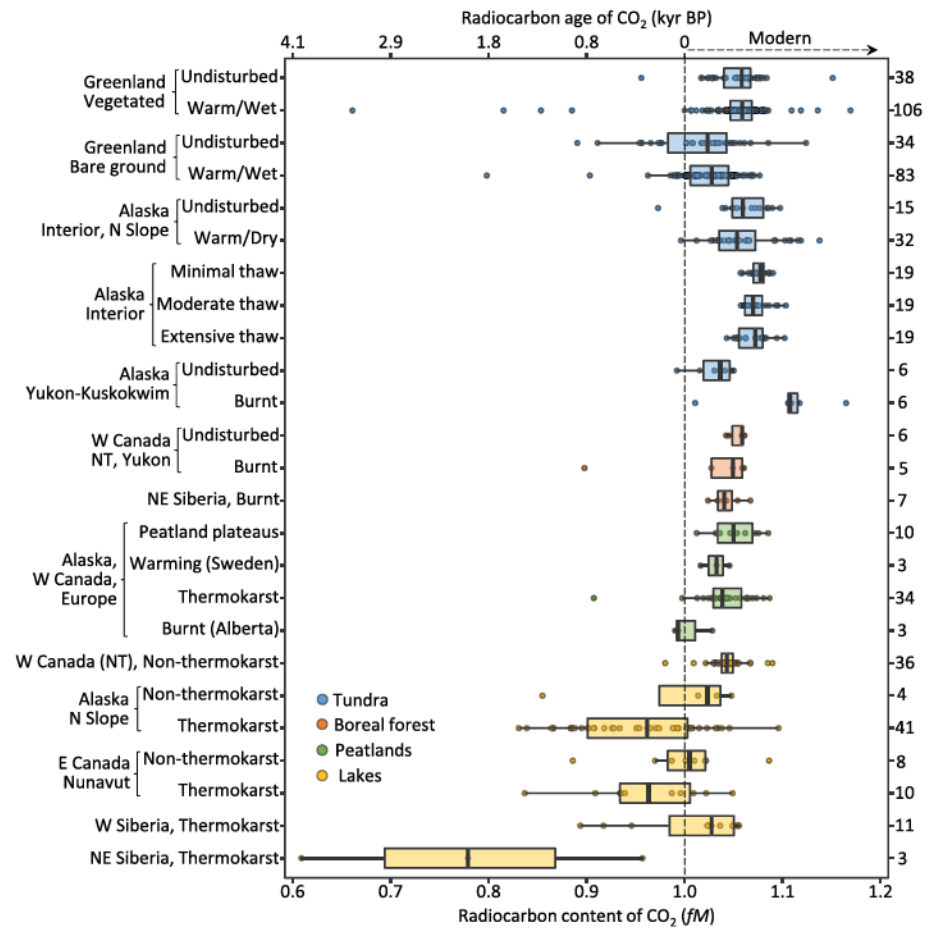


**Figure 4.** Radiocarbon content of  $\text{CO}_2$  emissions in the northern permafrost region. Data show  $\text{CO}_2$  flux measurements and exclude belowground and soil incubation measurements. Data are grouped by combining site location, experimental treatments, and types of disturbance shown on the left. The boxes show the first and third quartiles, the solid vertical line is the median, and the whiskers extend 1.5 times the interquartile range. Each point shows a  $^{14}\text{C}$  measurement and the total number of measurements is shown on the right.

### 3.4. Carbon Dioxide Emissions

The  $^{14}\text{C}$  values of  $\text{CO}_2$  emissions in tundra sites with field manipulations (soil warming, wetting, and drying in Greenland and Alaska) did not show a consistent pattern compared to undisturbed sites and were dominated by modern C (Figure 4). Nevertheless, while  $^{14}\text{C}$ - $\text{CO}_2$  emissions on their own did not indicate differences in the age of  $\text{CO}_2$  following these disturbances (Figure 4), belowground in situ measurements did consistently show lower  $^{14}\text{C}$ - $\text{CO}_2$  in manipulated compared to undisturbed sites (Greenland and Alaska in Figure 5). Soil pore space  $\text{CO}_2$  was clearly more depleted in  $^{14}\text{C}$  in manipulated than undisturbed tundra, especially in warmer and drier treatments, highlighting the importance of both temperature and moisture in regulating the age of SOC being decomposed in these ecosystems. Higher  $^{14}\text{C}$ - $\text{CO}_2$  values in the burnt versus undisturbed locations in Alaska Yukon-Kuskokwim (Figure 4) could result from fire having removed organic matter from the profile without combusting soil layers with bomb  $^{14}\text{C}$  and this source becoming more prominent in the flux. We found a consistent pattern of lower  $^{14}\text{C}$ - $\text{CO}_2$  emissions among well-drained sites where the active layer was deepening compared to undisturbed locations. This pattern was observed in tundra (interior Alaska), dominated by modern values, and in burned boreal forest (W Canada) and burned peat plateau (Alberta) where values were occasionally premodern (Figure 4). Soil pore space  $\text{CO}_2$  was also more depleted in  $^{14}\text{C}$  in the burnt forest and peat plateaus compared to the undisturbed locations (Figure 5). Overall, these observations in well-drained sites indicated a detectable influence of thaw



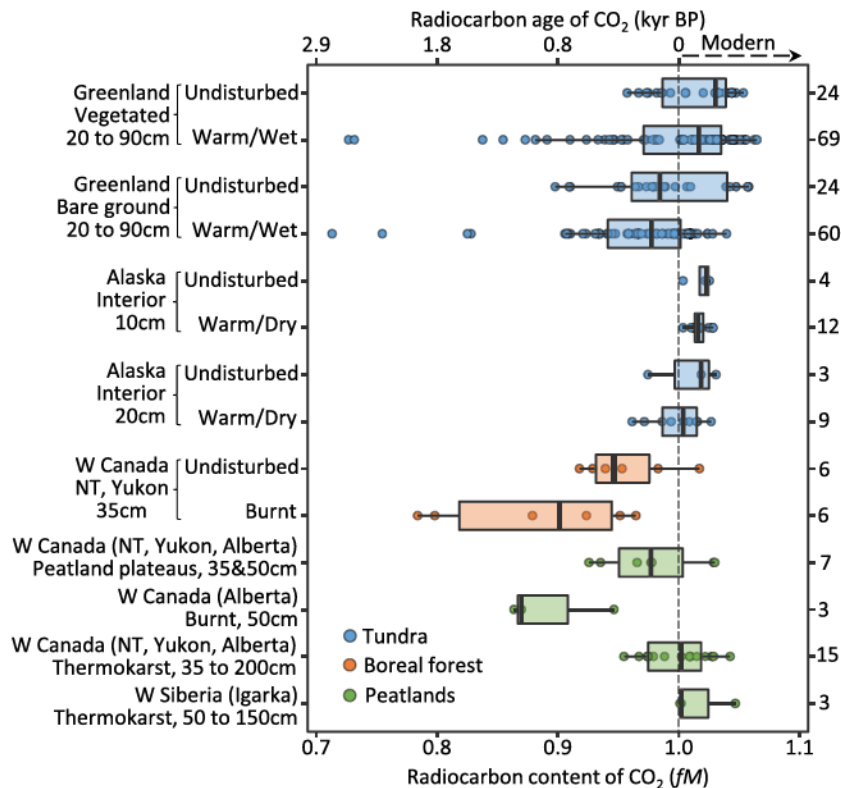


**Figure 5.** Radiocarbon content of belowground  $\text{CO}_2$  collected in situ at depth in soils in the northern permafrost region (no incubation measurements included, for incubations data refer to Figures S2 and S3). The boxes show the first and third quartiles, the solid vertical line is the median, and the whiskers extend 1.5 times the interquartile range. Each point shows a  $^{14}\text{C}$  measurement and the total number of measurements is shown on the right.

on the age of  $\text{CO}_2$  released and showed an overall increase of mineralization of deep SOC following disturbance in oxic soils during the growing season (Table 2), especially when active layer deepening affected SOC-rich layers.

In contrast to terrestrial ecosystems with oxic soils, we found that thermokarst peatlands with anoxic soils did not have an increased release of thawed SOC compared to undisturbed peatland plateaus. Thermokarst peatlands in Alaska and W Canada showed that  $\text{CO}_2$  fluxes were largely dominated by modern C (Figure 4) despite these ecosystems having two to six times greater thawed SOC mass than nearby permafrost peat plateaus with basal peats dating around ~8,000 years BP. In addition, and contrasting with the rest of belowground observations in well-drained soils from tundra and boreal forest, soil pore space measurements did not reflect more depleted  $^{14}\text{C}$ - $\text{CO}_2$  in thermokarst bogs compared to undisturbed or burnt peat plateaus (Figure 5). Indeed, “old” SOC mineralization was reported to be lower in thermokarst peatlands compared to adjacent undisturbed peatland plateaus (Table 2).

$\text{CO}_2$  emissions from lakes and ponds were mostly modern in nonthermokarst and premodern in thermokarst systems. The only comparison possible regarding disturbance effects also indicated premodern  $\text{CO}_2$  emissions in thermokarst lakes and ponds, and modern values in nonthermokarst sites (Alaska and E Canada, Figure 4). However, premodern  $\text{CO}_2$  release was also observed in nonthermokarst lakes/ponds where sampling was more limited. The age of the  $\text{CO}_2$  released from thermokarst lakes was overall much younger than the organic matter in the sediments, as observed in N Slope of Alaska, W Siberia, and E Siberia, which suggests that in-lake processes were particularly important for  $\text{CO}_2$  as it has a reasonably high component sourced from the oxic water column and/or surficial (oxic) sediments. We did not find reported estimates of “old” C release comparing thermokarst and nonthermokarst locations (Table 2).

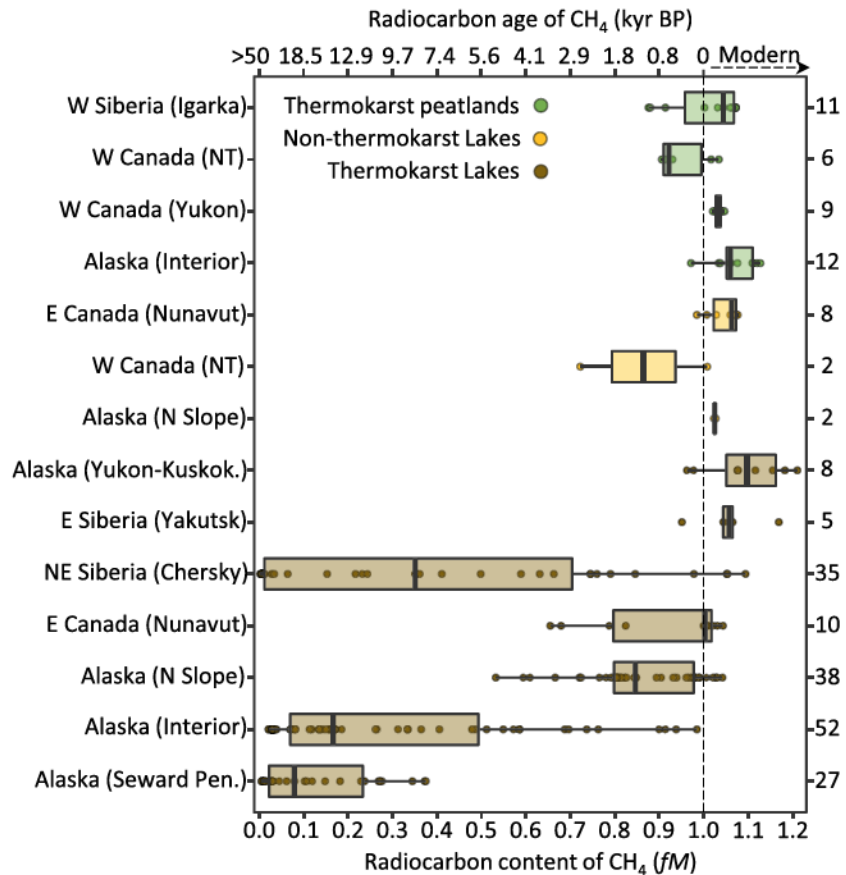


**Figure 6.** Radiocarbon content of  $\text{CH}_4$  released to the atmosphere in peatlands and lakes in the northern permafrost region. Data shown in this figure include diffusive and ebullitive fluxes (no belowground measurements included). The boxes show the first and third quartiles, the solid vertical line is the median, and the whiskers extend 1.5 times the interquartile range. Each point shows a  $^{14}\text{C}$  measurement and the total number of measurements is shown on the right.

We found extensive evidence across ecosystems that seasonality influences the contribution of deeper SOC to soil  $\text{CO}_2$  respiration. Most data showed an increasing contribution of older sources with the seasonal thawing of the active layer as the growing season progressed (Dean et al., 2018; Hicks Pries et al., 2013; Klapstein et al., 2014; Schuur et al., 2009).

### 3.5. Methane Emissions

The age of  $\text{CH}_4$  released from thermokarst peatlands was mostly modern as shown in measurements from ebullition in Alaska and W Siberia, and from diffusive fluxes in W Canada although premodern values up to ~1,000 years BP were also observed (Figure 6). Modern  $\text{CH}_4$  when water table remained high (W Canada, Yukon) contrasted with premodern  $\text{CH}_4$  values during a summer drought that lowered the water table (W Canada, NT). While drought increased the contribution of deep SOC aged 1,200 years BP to  $\text{CH}_4$  emissions (Table S2), this higher contribution was associated with much lower  $\text{CH}_4$  emissions and the overall absolute release of such aged SOC as  $\text{CH}_4$  remained low regardless of the water table level (Table 2).

We found a large variability in the age of  $\text{CH}_4$  emissions in thermokarst lakes (modern to >50 kyr BP) (Figure 6), which was related to the variability in the age of SOC. Thermokarst lakes in basins underlain by Yedoma soils in regions of NE Siberia and Alaska released modern to Pleistocene-aged  $\text{CH}_4$  whereas measurements in non-Yedoma regions generally showed modern to ~3,000 years BP  $\text{CH}_4$  release. The distinction between first- and second-generation thermokarst lakes (Brosius et al., 2012) determined the age of sediments available to mineralization following thaw in our data set; first-generation thermokarst lakes

resulted from the thaw of ice-rich Pleistocene sediments whereas second-generation thermokarst lakes resulted from the thaw of sediments deposited during the Holocene. The oldest  $\text{CH}_4$  release was largely observed in first-generation thermokarst lakes from regions with extensive Pleistocene-aged ice-rich sediments (Yedoma), such as NE Siberia, the Seward Peninsula of Alaska, or in interior Alaska (Figure 6). In contrast, modern to 300 years BP  $\text{CH}_4$  occurred in second-generation thermokarst lakes near Yakutsk in E Siberia and Yukon-Kuskokwin in Alaska despite these regions being expected to contain substantial Pleistocene-aged sediments. Additionally, measurements in Yukon-Kuskokwin and E Siberia basins were collected from locations with abundant vegetation which suggests that relatively high lake productivity most likely contributed toward modern  $\text{CH}_4$  release (Figure 6).

The age of  $\text{CH}_4$  emissions from lakes was also influenced by whether emissions were associated with diffusion or ebullition. The age of  $\text{CH}_4$  in bubbles was much older in high-emission point locations (11 to 43 kyr BP) compared to low-emission locations (<9 kyr BP) or to bubbles from stirred surface sediments (<4 kyr BP). Noteworthy, these  $^{14}\text{C}$ - $\text{CH}_4$  ebullition observations come from limited measurements in a few lakes in most regions: two main lakes and a small undetermined number of additional lakes in NE Siberia ( $n = 35$ ), three lakes in the Seward Peninsula in Alaska ( $n = 27$ ), and 11 lakes in interior Alaska ( $n = 52$ , 30 of which from a single lake). A more extensive sampling in more than 30 lakes with Pleistocene-aged deposits across the N Slope in Alaska showed much younger diffusive  $\text{CH}_4$  fluxes (modern to 3,300 years BP) (Figure 6). Importantly, reported losses of “old” SOC as  $\text{CH}_4$  in N Slope Alaska were at least an order of magnitude lower than in NE Siberia and two orders of magnitude lower than those of  $\text{CO}_2$  (Table 2).

Only a few studies reported both the age of  $\text{CO}_2$  and  $\text{CH}_4$  (Figure S4). The limited available data indicated younger  $\text{CO}_2$  than  $\text{CH}_4$  in lakes (from 400 years BP in N Slope Alaska and up to 3,000 years BP younger in Nunavut, Figure S4a). The opposite trend was observed in trough ponds, polygonal ponds, and thermokarst peatlands with up to 780 years BP older  $\text{CO}_2$  than  $\text{CH}_4$  (Figure S4a).

### 3.6. DOC and POC Export

Pore waters from Yedoma soil and waters from Yedoma thaw streams showed the most depleted  $^{14}\text{C}$  values and were the clearest example of previously frozen C being mobilized as DOC and POC (Figures 7 and 8). High DOC and POC concentrations (Figure S5) with ages between 9,600 and 38,300 years BP occurred in thaw streams directly draining slumps of late Pleistocene tills and early Pleistocene Yedoma deposits in W Canada and NE Siberia, respectively. Despite this, modern values largely dominated in DOC samples from tributaries and main stem of the Kolyma River (Figure 7) which drain landscapes with abundant thermokarst features.

In peatlands, pore water samples indicated substantially more depleted  $^{14}\text{C}$ -DOC in peat plateaus (burnt or intact) than in adjacent thermokarst peatlands in W Canada, although low  $^{14}\text{C}$  values were also observed in pore waters from thermokarst peatlands in W Siberia (Figure 7). Streams draining burnt peatlands in the Taiga Plains in W Canada had lower  $^{14}\text{C}$ -DOC than those in an undisturbed catchment (Figure 7), but the difference was relatively low and the C flux was generally dominated by modern DOC regardless of disturbance (Burd et al., 2018). Overall, blackwater rivers in the Yukon River Basin represent watersheds dominated by peatlands and generally yielded modern DOC (Figure 7), which suggests that depleted  $^{14}\text{C}$ -DOC in peat pore waters contributed marginally to DOC export.

Streams originating from glaciers showed substantially depleted  $^{14}\text{C}$ -DOC with ages up to 10 kyr BP in their headwaters, as shown in the Gulf of Alaska and in glacial waters in the Yukon River (Figure 7). Depleted  $^{14}\text{C}$ -DOC was also observed in glaciated catchments and nonglacial clearwaters in the Yukon River (Figure 7), a feature likely associated with the influence of  $^{14}\text{C}$  dead geologic sources.

The  $^{14}\text{C}$ -DOC in the main stem of large Arctic Rivers was largely dominated by modern C with a consistent change in age between seasons, tightly coupled to water discharge (Figure 7). With 50–80% of the annual DOC export typically occurring within 2 months of the spring freshet (Finlay et al., 2006; Holmes et al., 2012), the spring flood yields a large export of modern DOC derived from litter and surface soils upon the onset of thaw (Raymond et al., 2007). The bulk of DOC also remained dominated by modern sources throughout the year in middle- to high-order rivers, but the  $^{14}\text{C}$ -DOC signature decreased from spring to winter.



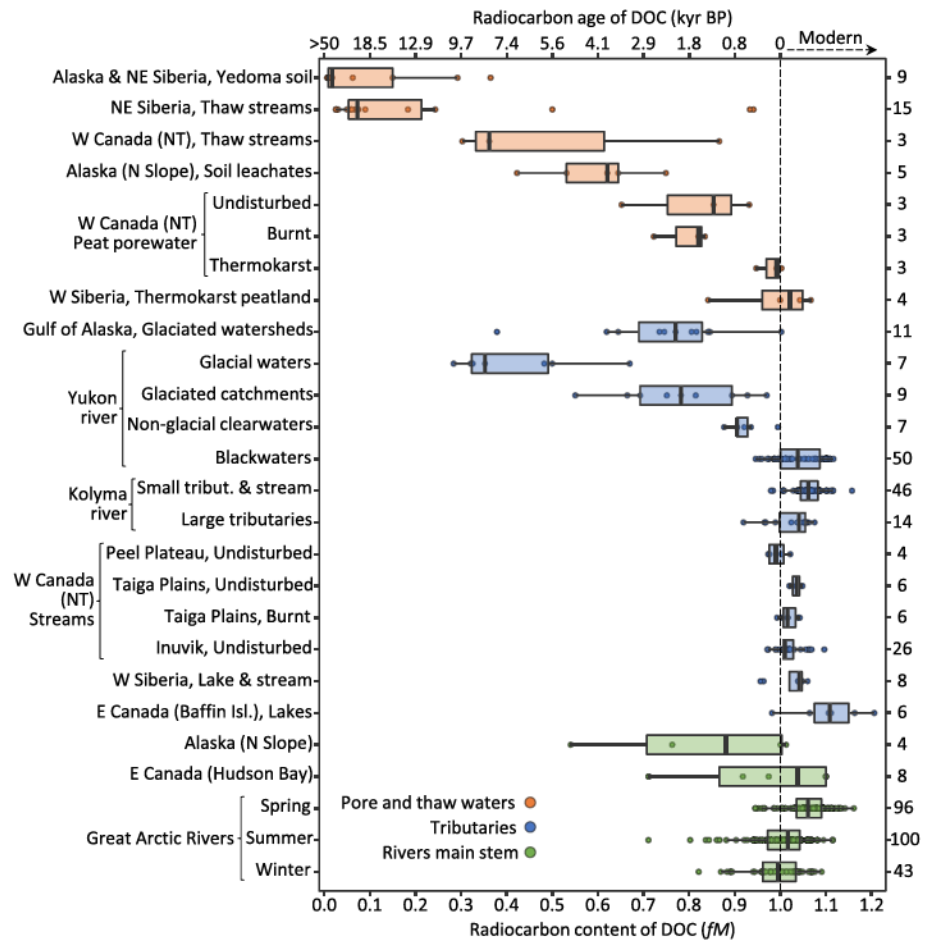


**Figure 7.** Radiocarbon content of DOC in the northern permafrost region. The boxes show the first and third quartiles, the solid vertical line is the median, and the whiskers extend 1.5 times the interquartile range. Each point shows a  $^{14}\text{C}$  measurement and the total number of measurements is shown on the right.

Riverborne POC was overall substantially more depleted in  $^{14}\text{C}$  than DOC (Figure 8). POC age had generally less variability over seasons compared to DOC in large Arctic rivers, except for more depleted  $^{14}\text{C}$ -POC observed with increasing water yield in the Mackenzie river (Figure 8; McClelland et al., 2016). Comparing the  $^{14}\text{C}$  of POC and DOC among the largest Arctic Rivers showed a smaller difference in the age between both C forms in the Ob', Yenisey, and Lena rivers compared to the Yukon, Mackenzie, and Kolyma rivers (Figure S4c).

#### 4. Discussion

Radiocarbon provides insights about the mobilization and fate of thawed SOC following disturbance. Our synthesis of reported  $^{14}\text{C}$  data from the northern permafrost region has identified ecosystems where aged SOC is released in different forms, and below we will discuss the role of active layer deepening, thermokarst, and aquatic C export. In summary, our review of the available literature shows that the key factors identified as influencing the  $^{14}\text{C}$  signature of C fluxes included SOC properties such as SOC age and content, soil thermal dynamics (thaw depth and temperature), fraction of the soil profile water-saturated, influence of primary production, distance from points of thermal erosion in stream networks, incorporation of other sources than SOC in the bulk pool, and seasonality. Overall, we found strong  $^{14}\text{C}$ -based evidence of increased release of older SOC sources following thaw in SOC-rich terrestrial ecosystems that remain well-drained, in actively expanding thermokarst lakes, and in headwaters with active thermal erosion (Figure 9).

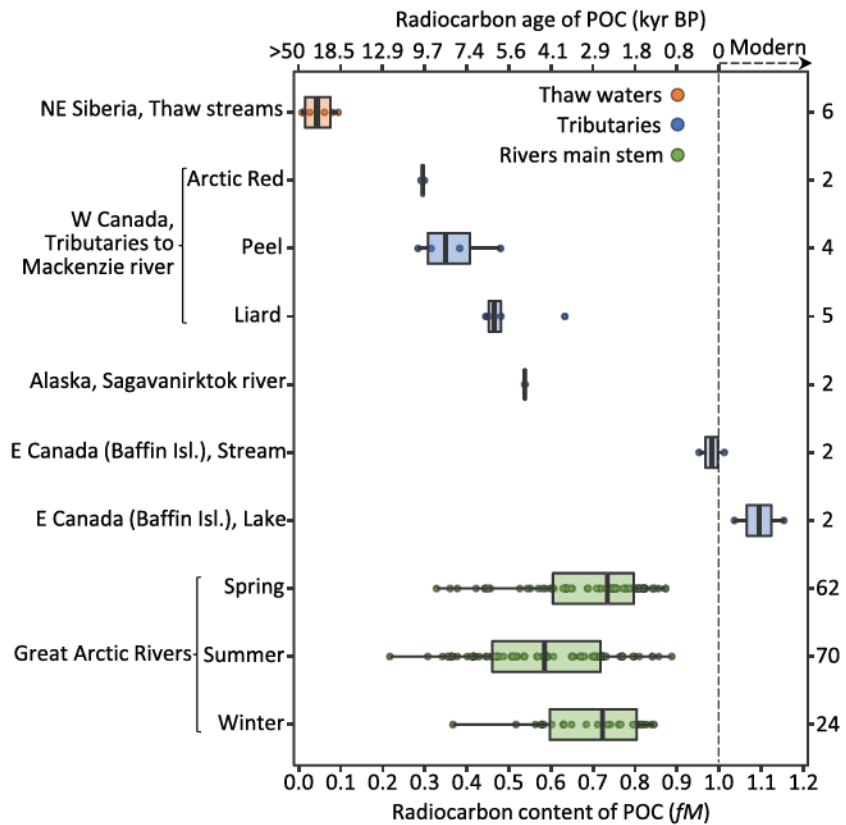


**Figure 8.** Radiocarbon content of POC measured in the northern permafrost region. The boxes show the first and third quartiles, the solid vertical line is the median, and the whiskers extend 1.5 times the interquartile range. Each point shows a  $^{14}\text{C}$  measurement and the total number measurements is shown on the right.

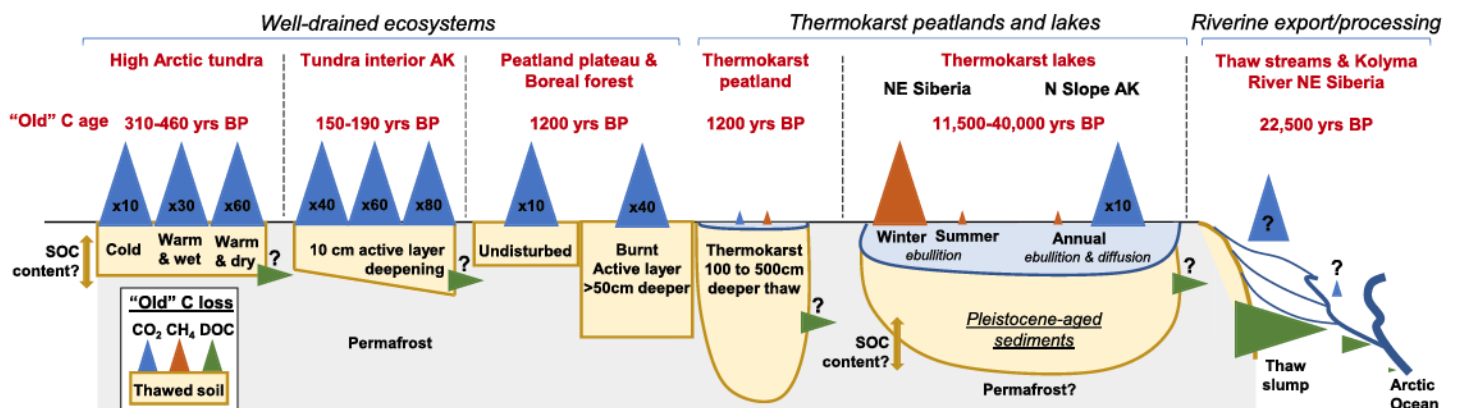


**Figure 9.** Vulnerability of "old" SOC across ecosystems in the northern permafrost region. We highlight the effects of thaw by active layer deepening (well-drained ecosystems), thermokarst (water-logged ecosystems), and thaw slumps through thermal erosion (riverine export). Sizes of the arrows and the factor shown in them for  $\text{CO}_2$  and  $\text{CH}_4$  depict relative fluxes of "old" C estimated across ecosystems by different studies (refer to Table 2 for flux values). Note that each ecosystem had its own defined age of "old" C. Thus, the flux of "old"  $\text{CO}_2$  is similar for High Arctic tundra and for thermokarst lakes in N Slope AK (same arrow size with a factor of  $\times 10$ ) but the age of "old" C was either 310–460 or 11,500–40,000 years BP, respectively. The arrow size for DOC shown in green indicates relative proportions of "old" C and is not comparable to the arrows for gas C release but rather reflects processing along the stream network. Arrows with question marks indicate unknown rates. Note that for thermokarst lakes in NE Siberia there is no reported  $\text{CO}_2$  loss and winter  $\text{CH}_4$  release occurs during the spring thaw after it accumulates under ice cover over autumn and winter.

#### 4.1. Active Layer Deepening in Well-Drained Ecosystems

The available data showed generally greater mineralization of older SOC sources following increased thaw in well-drained sites (Figure 9). More depleted  $^{14}\text{C}$ - $\text{CO}_2$  emissions were apparent when thaw affected a sufficient fraction of soil with a relatively high SOC content in well-drained sites. This occurred in sites with a SOC stock of at least  $50 \text{ kg C m}^{-2}$  to 1 m depth when the active layer increased by  $<10 \text{ cm}$  across a thaw gradient in tundra interior Alaska and by  $>50 \text{ cm}$  in burned forest and burned peat plateau (Figure 9). On the other hand, more depleted  $^{14}\text{C}$ - $\text{CO}_2$  emissions were not observed in tundra sites with a lower SOC stock ( $<10 \text{ kg C m}^{-2}$  warm/wet in Greenland in Figure 4) or which experienced a smaller increase in thaw depth ( $\approx 3 \text{ cm}$  in warming in interior Alaska in Figure 4), although depleted  $^{14}\text{C}$ - $\text{CO}_2$  in the soil pore space suggests increased mineralization of older SOC sources taking place (Figure 5). Overall, these results indicate well-drained sites have a large potential for permafrost SOC mineralization depending on the extent of thaw, SOC content, and degree of water saturation in deep soil layers (Estop-Aragonés, Cooper, et al., 2018; Estop-Aragonés, Czimczik, et al., 2018; Hicks Pries et al., 2013; Lupascu, Welker, Seibt, et al., 2014; Natali et al., 2015; Schuur et al., 2009). Active layer deepening in SOC-rich ecosystems is thus expected to increase mineralization of previously frozen SOC with the potential for rapid release following fire-induced, as well as in response to gradual thaw.

#### 4.2. Anoxic Ecosystems Developed Through Thermokarst

The compiled  $^{14}\text{C}$  data indicated younger  $\text{CO}_2$ ,  $\text{CH}_4$ , and DOC in thermokarst peatlands than in peat plateaus and limited mineralization of previously frozen SOC in thermokarst peatlands compared to the adjacent undisturbed peat plateaus (Figure 9). This suggests greater mobilization of previously frozen SOC when the mode of thaw is active layer deepening and soils presumably remain well-drained and oxic compared to waterlogged anoxic conditions following thermokarst in peatlands. The predominantly modern C observed in thermokarst peatlands suggests that vegetation growing postthaw strongly influences C cycling in these ecosystems. The rapid vegetation growth and peat accumulation following thaw in thermokarst peatlands (Camill, 1999; Estop-Aragonés, Cooper, et al., 2018; Turetsky et al., 2000; Wilson et al., 2017) could explain the low contribution of older SOC sources to the flux, if  $\text{CO}_2/\text{CH}_4/\text{DOC}$  emissions are dominated by sources derived from such recent and labile C inputs due to downward transport in the soil profile. However, it is unclear how a potential supply of labile C can explain why absolute rates of “old” SOC release are lower in thermokarst peatlands than in undisturbed peat plateaus (Table 2), despite thaw exposing tens of kilograms of previously frozen C per  $\text{m}^2$ . It appears that in these ecosystems, long-term exposure to anoxic conditions reduces rates of peat decomposition by a much greater magnitude than predicted in anaerobic laboratory incubations (Treat et al., 2015). The contribution of previously frozen SOC was estimated to represent about half of the total  $\text{CO}_2$  production in short-term anaerobic incubations but these sources were barely detectable in situ (Estop-Aragonés, Cooper, et al., 2018). The accumulation of end products of decomposition in waterlogged peatlands is argued to thermodynamically limit further decay (Beer & Blodau, 2007; Blodau et al., 2011). This may occur when the energy available in the environment during anaerobic organic matter decomposition is comparable to the energy conserved by microbes and thus, thermodynamic factors reduce or even inhibit respiration (Jin & Bethke, 2005).

In contrast to the modern C flux in thermokarst peatlands, there was a large variability in the age of C released from thermokarst lakes (from modern to  $>50 \text{ kyr BP}$ ). This variability was largely related to factors such as age and organic C content of sediments and to whether thermokarst lakes were expanding or not (Elder et al., 2018; Walter et al., 2008). Other factors such as sampling location and season and lake size/depth clearly influenced the relative contribution of fresh inputs versus older sources (Bouchard et al., 2015; Elder et al., 2018; Martens et al., 1992; Walter Anthony et al., 2016). The difference between the  $^{14}\text{C}$  of  $\text{CO}_2$  and  $\text{CH}_4$  emitted from thermokarst peatlands and lakes may be due to differences in productivity and thus rate of decomposition of recent, labile plant material. The contribution of modern sources to  $\text{CO}_2$  and  $\text{CH}_4$  fluxes is undoubtedly lower in thermokarst lakes, which are much less productive given the water column typically exceeds depths preferred by emergent vegetation in thermokarst peatlands. Such lower plant productivity in thermokarst lakes combined with far faster talik growth rates (Walter Anthony et al., 2018) could explain why previously frozen SOC sources contributed more to  $\text{CO}_2$  and  $\text{CH}_4$  release in lakes than in peatlands despite the prevailing anoxic conditions in both ecosystems following thermokarst development. The younger  $\text{CO}_2$  than  $\text{CH}_4$  in lakes but the opposite trend in ponds and thermokarst



peatlands (Figure S4a) could also be related to greater productivity driving modern CH<sub>4</sub> production in ecosystems with a relatively higher terrestrial influence (trough ponds, polygonal ponds, and thermokarst peatlands). Another important factor in lakes is that primary producers may fix dissolved inorganic carbon (not atmospheric CO<sub>2</sub>) from the water column and produce older organic C sources that can be further cycled, which may result in an overall older lacustrine C pool, i.e., a reservoir effect (Abbott & Stafford, 1996). Nevertheless, we lack a mechanistic understanding about the contrasting mineralization of previously frozen SOC between thermokarst peatlands and thermokarst lakes and it is unclear if factors such as nutrient content or sediment chemistry may influence SOC decomposition through, e.g., the build-up of inhibitory compounds. Overall, key differences that likely explain the observed differences in age of CO<sub>2</sub> and CH<sub>4</sub> between peatlands and lakes in our data set include (1) Holocene-aged SOC accumulated in peatlands versus Pleistocene-aged SOC in some lakes reported here and (2) higher and more spatially homogeneous productivity in peatlands than in lakes, where sample location (edge versus center) might determine the influence of primary production and, thus, of CO<sub>2</sub> and CH<sub>4</sub> age.

A striking feature in our data set is the potential for Pleistocene-aged SOC release as CH<sub>4</sub> through ebullition in some thermokarst lakes. Overall, the age of CH<sub>4</sub> released as bubbles was strongly related to the age of the soil deposit in thermokarst lakes (refer to Figure 2b in Walter Anthony et al., 2016). While substantial, such thermokarst lake data were mostly focused on <sup>14</sup>C-CH<sub>4</sub> and in specific locations within the Yedoma region, and thus targeted to detect sources of older SOC sources (Walter Anthony et al., 2016; Zimov et al., 1997). It is unclear if this is skewing our understanding of the vulnerability of permafrost SOC in these ecosystems given that (1) the non-Yedoma region may store more permafrost SOC overall (Strauss et al., 2017) and (2) lake C emissions seem to be dominated by CO<sub>2</sub> through diffusive fluxes and by relatively limited contribution of Yedoma sources in other regions with Pleistocene-aged sediments (Elder et al., 2018; Nakagawa et al., 2002). Additional measurements in nonthermokarst lakes are also required to compare against the <sup>14</sup>C data in thermokarst lakes and better assess the vulnerability of permafrost SOC following disturbance.

#### 4.3. Mobilization and Processing of DOC and POC in Aquatic Networks

Modern DOC largely dominated in tributaries and main stem of rivers even in Yedoma landscapes that released high concentrations of Pleistocene-aged DOC. This lack of depleted <sup>14</sup>C signatures in the bulk DOC downstream could be explained by the high lability of ancient DOC (Spencer et al., 2015; Vonk et al., 2013) with a preferential decomposition of the older C fraction shown in incubations (Mann et al., 2015). In this regard, DOC in thaw waters from similar ice-rich Yedoma soils in Alaska is shown to contain 30% of labile substrates (mainly acetate) (Ewing et al., 2015), which adds to the potential reactivity of these highly DOC concentrated water samples of Pleistocene age (Abbott et al., 2014; Drake et al., 2015; Vonk et al., 2015). Together, these findings suggest that DOC measurements in middle- to higher-order rivers may be unsuitable to detect mobilization of thawed SOC, which may have been preferentially mineralized in headwater streams.

The seasonal trend in <sup>14</sup>C-DOC in middle- to high-order rivers suggests an increasing contribution of older SOC sources during the growing season as thaw depth increases and subsurface flow paths are routed through deeper soils (Barnes et al., 2018; O'Donnell et al., 2012; Toohey et al., 2016). Such seasonality in <sup>14</sup>C-DOC was accompanied by a change in DOC composition, as reflected by decreasing DOC aromaticity from spring to winter in the Yukon and Kolyma Rivers (Aiken et al., 2014; Neff et al., 2006; O'Donnell et al., 2014; Striegl et al., 2007). The shift in both age and composition of DOC with season likely reflects a number of processes, including increasing microbial mineralization of modern, labile DOC compounds with warmer temperatures (O'Donnell et al., 2016), preferential sorption of aromatic compounds by reactive mineral surfaces (Kawahigashi et al., 2004, 2006), and shifting DOC source from near-surface SOC to deeper SOC and microbial by-products (Barnes et al., 2018; O'Donnell et al., 2012). Recognizing that measurements in the main stem of rivers do not account for the abovementioned potential loss of permafrost-derived sources upstream, 95% of DOC export in spring was derived from C fixed within the last 20 years (Raymond et al., 2007). In spring, little permafrost SOC is expected to be transiting to streams despite the major export of labile DOC (Holmes et al., 2008). This outcome can arise because only the shallowest part of the active layer is thawed, and both short residence times and low temperatures potentially prevent mineralization (Raymond et al., 2016). Given the low DOC concentrations during base flow conditions in winter, the overall absolute mobilization of permafrost SOC as DOC to the Arctic Ocean is thus

considered limited in large rivers (Raymond et al., 2007). By contrast, mineralization and processing of such sources may be dominant in headwaters (Drake et al., 2015). Considering the annual DOC export to the Arctic Ocean is only about 25 Tg C (Holmes et al., 2012), quantifying the extent of thawed SOC lost as CO<sub>2</sub> in headwater streams is important to determine if permafrost-derived DOC represents a globally important flux. Measurements in situ of <sup>14</sup>C-CO<sub>2</sub> in thaw streams and other disturbed ecosystems are thus required (Figure 9) to better couple the large DOC losses reported in some studies to greenhouse gas production, which are currently inferred from incubation data (Drake et al., 2018; Mann et al., 2015; Spencer et al., 2015).

Glacial and geological sources other than SOC likely affected freshwater <sup>14</sup>C-DOC and <sup>14</sup>C-POC in certain landscapes and these sources need to be accounted for to detect permafrost SOC export. Glacier-derived DOC depleted in <sup>14</sup>C in the Gulf of Alaska (Hood et al., 2009) was strongly influenced by anthropogenic fossil fuels deposited as aerosols on the glaciers (Stubbins et al., 2012), and thus did not reflect SOC age. Additionally, assimilation of <sup>14</sup>C dead geologic sources into organic matter results in apparent <sup>14</sup>C-DOC ages older than the time of assimilation, i.e., a reservoir effect (Fellman et al., 2015; Philippsen, 2013). This phenomenon included dissolved suspended carbonates in waters draining alpine and glacial environments (glaciated catchments in Figure 7) and shales and coals in groundwater-influenced waters (nonglacial clearwaters in Figure 7) in the Yukon River and Arctic watersheds in Baffin Island (Abbott & Stafford, 1996; Aiken et al., 2014). Similarly, somewhat older POC in the Mackenzie River may be attributed to a higher petrogenic component (<sup>14</sup>C dead bitumens and kerogens) (Goñi et al., 2005).

While DOC is the dominant fraction of total organic carbon exported to the Arctic Ocean (McClelland et al., 2016; Raymond et al., 2007), POC showed much more depleted <sup>14</sup>C content. Young DOC but extremely old POC observed in Arctic rivers is consistent with experimental results that show only a small fraction (<2%) of SOC can be released into the DOC pool during permafrost interactions with aquatic environments (Gao et al., 2018; Xu et al., 2009). Riverborne POC at high latitudes was generally derived from the erosion of river banks and other near-stream soils, and the <sup>14</sup>C of POC typically reflects the age of eroded soils (Guo et al., 2007). The smaller difference in age between DOC and POC in the Ob', Yenisey, and Lena rivers agrees with the lower mean slope in these rivers (Amon et al., 2012), and thus lower potential for erosion, in comparison to the Yukon, Mackenzie, and Kolyma rivers, where river bank erosion may be greater and favor older POC export from deeper layers. Indeed, the lowest difference was observed in the Ob' river, which has the lowest slope and greatest peatland coverage. Compared to other major Siberian Arctic rivers, somewhat older POC in the Kolyma River may be attributed to greater contributions of Pleistocene-aged SOC (Yedoma) (Wild et al., 2019). Importantly, it is unclear to what extent the increased export of permafrost SOC as POC results in a positive feedback to the climate. A characterization of sources and fate of POC along the Mackenzie River (Figure 8) showed that while an increase in erosion may cause more POC mobilization from permafrost sources, such effects may actually result in an increased CO<sub>2</sub> sink in the long-term considering the potential for C burial in marine sediments (Hilton et al., 2015). Further quantification of POC mineralization rates during transport in other rivers and in the depositional environment is required to determine the extent to which POC fluxes derived from permafrost may actually represent a CO<sub>2</sub> source.

#### 4.4. Opportunities and Challenges for Future <sup>14</sup>C Studies

Determining the fate and loss rate of previously frozen SOC should be prioritized in future <sup>14</sup>C studies to quantify the current permafrost C-climate feedback. We found there is no standard approach to quantifying the rate of "old" SOC release (Table S2), which complicates the comparison between studies. There is also some inconsistency in ways this term is used to refer to the sources of C released in relation to the permafrost C-climate feedback since "old" SOC may or may not refer to permafrost or previously frozen C sources in the literature. Given that the SOC age continuum extending from the soil surface downward may differ greatly across ecosystems and landscapes, the age of permafrost SOC can be a few centuries to millennia in areas with rapid C accumulation or shallow permafrost, or tens of millennia in areas with Pleistocene deposits. We emphasize that linking ecosystem <sup>14</sup>C fluxes to SOC stocks available for mineralization is urgently needed. We advocate reporting the estimated mass of SOC stocks thawed per unit area and expressing loss rates of previously frozen SOC sources per unit of SOC stocks thawed, e.g., mass of permafrost C released to the atmosphere as CO<sub>2</sub> or CH<sub>4</sub> per mass of thawed SOC per unit area and time. This would increase



substantially the potential for comparing between studies and help determine the vulnerability of SOC across ecosystems with different glacial histories and/or different types of disturbance.

Targeted  $^{14}\text{C}$  sampling is required in some ecosystems and from certain types of disturbance. Most  $^{14}\text{C}$  data clustered in a few sites and were often sampled during limited periods of the year, mostly during the growing season, which makes it difficult to know how representative such findings are in a wider spatial and temporal scale (Metcalf et al., 2018). Regarding spatial gaps, almost no  $^{14}\text{C}$  data exists in most of Siberia and E Canada despite the large permafrost SOC stock stored in the Hudson Bay Lowlands and the West Siberian Lowlands, and regions with abundant lakes such as the Canadian Shield. The lack of in situ  $^{14}\text{C}$  measurements of  $\text{CO}_2$  in terrestrial ecosystems in Siberia is particularly striking. This gap is particularly important to close as we showed that fire-induced active layer deepening is likely a major path for permafrost SOC release as  $\text{CO}_2$  in well-drained soils based on the few estimates from boreal forest and peatlands in W Canada. Regarding temporal gaps, the importance of fall and winter periods for annual permafrost SOC mineralization is poorly documented in most ecosystems. Further sampling during the spring thaw in lakes and peatlands is also required to characterize the potential pool of deep SOC mineralized and accumulated during the freeze period and that is released during such short events (Figure 9).

The link between DOC and  $\text{CO}_2$  will likely gain importance in the near future as warming and thaw increase connectivity between aquatic and terrestrial landscapes. We found a general lack of simultaneous  $^{14}\text{C}$  measurements among different C forms with the exception of few studies (Bouchard et al., 2015; Dean et al., 2018; Dutta et al., 2006; Elder et al., 2018; Klapstein et al., 2014) (Figure S4). A suite of simultaneous in situ  $^{14}\text{C}$  measurements could help to link POC and DOC degradation to  $\text{CO}_2$  and  $\text{CH}_4$  production (Dean et al., 2020) to determine how widespread is the abovementioned preferential decomposition of the aged DOC fraction, i.e., is all “old” DOC labile? In this regard, there are very limited measurements linking  $^{14}\text{C}\text{-CO}_2$  and  $^{14}\text{C}\text{-DOC}$  in terrestrial and aquatic ecosystems, despite the importance of  $\text{CO}_2$  evasion from inland waters (Regnier et al., 2013; Tank et al., 2018) and despite older  $\text{CO}_2$  being shown to be released from modern bulk DOC samples (Dean et al., 2019; McCallister & del Giorgio, 2012). This information is key as there is a need to calculate DOC and POC fluxes to compare them with greenhouse gas fluxes in order to determine the potential importance of the different pathways regarding permafrost SOC release.

Prolonged and continued  $^{14}\text{C}$  monitoring is particularly important to estimate permafrost SOC release in coming years. The few multiyear studies in tundra and the main stem of rivers have provided a better understanding of the control of weather extremes and soil environmental conditions on the variability of release of aged SOC sources (Lupascu, Welker, Seibt, et al., 2014; Raymond et al., 2007; Schuur et al., 2009). For example, decadal monitoring of  $^{14}\text{C}\text{-POC}$  reflected mobilization of permafrost SOC in the Kolyma River by thermokarst and erosion of Yedoma deposits (Wild et al., 2019). Our synthesis shows that it is difficult to conclude whether the SOC released from deep soils is generated because of landscape disturbance or is a normal component of terrestrial permafrost carbon cycling, given the lack of an appropriate baseline. Such effort could be better understood through continued  $^{14}\text{C}$  monitoring by determining the  $^{14}\text{C}$  offset of a carbon pool over time with respect to the atmospheric decline. Atmospheric  $^{14}\text{C}\text{-CO}_2$  is decreasing due primarily to dilution effects from the release of  $^{14}\text{C}\text{-dead C}$  from fossil fuel combustion and may have already reached  $fM < 1$  (Graven, 2015). An ecosystem in steady state, for instance, may decrease at a rate similar to the atmosphere whereas if previously frozen SOC (depleted in  $^{14}\text{C}$ ) is released at high rates, the offset between the  $^{14}\text{C}$  trends of the released C form and the atmosphere may change and be detected for interpretation. Here we provide an additional data set of added value for earth system modelers. By comparing modeled  $^{14}\text{C}$  fluxes against the field measurements provided in this data set, earth system modelers will be better able to assess whether models are accurately capturing the evasive and lateral fluxes of permafrost SOC.

### Data Availability Statement

The data set is open at <https://zenodo.org/record/3832031#.XsJ8vntCSU1> with DOI 10.5281/zenodo.3832031 and has also been included in the ISRaD repository (<http://www.soilradiocarbon.org>).



## Acknowledgments

Funding and support were provided by the Natural Science and Engineering Research Council of Canada, Discovery grant (RGPIN-2016-04688), and the Campus Alberta Innovates Program (CAIP). A. M. H. received funding from the ERC Horizon 2020 programme (grant 695101). This study was also assisted by the Permafrost Carbon Network, which was supported by NSF project #1331083 and #1931333 to E. A. G. S. The authors thank James W. McClelland for comments, which improved the manuscript.

## References

- Abbott, B. W., Jones, J. B., Godsey, S. E., Larouche, J. R., & Bowden, W. B. (2015). Patterns and persistence of hydrologic carbon and nutrient export from collapsing upland permafrost. *Biogeosciences*, 12(12), 3725–3740. <https://doi.org/10.5194/bg-12-3725-2015>
- Abbott, B. W., Baranov, V., Mendoza-Lera, C., Nikolakopoulou, M., Harjung, A., Kolbe, T., et al. (2016). Using multi-tracer inference to move beyond single-catchment ecohydrology. *Earth-Science Reviews*, 160, 19–42. <https://doi.org/10.1016/j.earscirev.2016.06.014>
- Abbott, B. W., Larouche, J. R., Jones, J. B. Jr., Bowden, W. B., & Balser, A. W. (2014). Elevated dissolved organic carbon biodegradability from thawing and collapsing permafrost. *Journal of Geophysical Research: Biogeosciences*, 119, 2049–2063. <https://doi.org/10.1002/2014JG002678>
- Abbott, M. B., & Stafford, T. W. (1996). Radiocarbon geochemistry of modern and ancient Arctic lake systems, Baffin Island, Canada. *Quaternary Research*, 45(3), 300–311. <https://doi.org/10.1006/qres.1996.0031>
- Aiken, G. R., Spencer, R. G. M., Striegl, R. G., Schuster, P. F., & Raymond, P. A. (2014). Influences of glacier melt and permafrost thaw on the age of dissolved organic carbon in the Yukon River basin. *Global Biogeochemical Cycles*, 28, 525–537. <https://doi.org/10.1002/2013GB004764>
- Amon, R. M. W., Rinehart, A. J., Duan, S., Louchouart, P., Prokushkin, A., Guggenberger, G., et al. (2012). Dissolved organic matter sources in large Arctic rivers. *Geochimica et Cosmochimica Acta*, 94, 217–237. <https://doi.org/10.1016/j.gca.2012.07.015>
- Amon, R. M. W., & Meon, B. (2004). The biogeochemistry of dissolved organic matter and nutrients in two large Arctic estuaries and potential implications for our understanding of the Arctic Ocean system. *Marine Chemistry*, 92, 311–330. <https://doi.org/10.1016/j.marchem.2004.06.034>
- Barnes, R. T., Butman, D. E., Wilson, H. F., & Raymond, P. A. (2018). Riverine export of aged carbon driven by flow path depth and residence time. *Environmental Science and Technology*, 52(3), 1028–1035. <https://doi.org/10.1021/acs.est.7b04717>
- Beer, J., & Blodau, C. (2007). Transport and thermodynamics constrain belowground carbon turnover in a northern peatland. *Geochimica et Cosmochimica Acta*, 71(12), 2989–3002. <https://doi.org/10.1016/j.gca.2007.03.010>
- Benner, R., Benitez-Nelson, B., Kaiser, K., & Amon, R. M. W. (2004). Export of young terrigenous dissolved organic carbon from rivers to the Arctic Ocean. *Geophysical Research Letters*, 31, L05305. <https://doi.org/10.1029/2003GL019251>
- Blodau, C., Siems, M., & Beer, J. (2011). Experimental burial inhibits methanogenesis and anaerobic decomposition in water-saturated peats. *Environmental Science and Technology*, 45(23), 9984–9989. <https://doi.org/10.1021/es201777u>
- Bouchard, F., Laurion, I., Preskennis, V., Fortier, D., Xu, X., & Whitticar, M. J. (2015). Modern to millennium-old greenhouse gases emitted from ponds and lakes of the Eastern Canadian Arctic (Bylot Island, Nunavut). *Biogeosciences*, 12(23), 7279–7298. <https://doi.org/10.5194/bg-12-7279-2015>
- Brosius, L. S., Walter Anthony, K. M., Grosse, G., Chanton, J. P., Farquharson, L. M., Overduin, P. P., & Meyer, H. (2012). Using the deuterium isotope composition of permafrost meltwater to constrain thermokarst lake contributions to atmospheric CH<sub>4</sub> during the last deglaciation. *Journal of Geophysical Research*, 117, G01022. <https://doi.org/10.1029/2011JG001810>
- Brown, J., Ferrians, O. J., Heginbottom, J. A., & Melnikov, E. S. (1997). *Circum-Arctic map of permafrost and ground-ice conditions*, Circum-Pacific Map Series. Washington, DC: U.S. Geological Survey.
- Brown, J., & Romanovsky, V. E. (2008). Report from the international permafrost association: State of permafrost in the first decade of the 21st century. *Permafrost and Periglacial Processes*, 19, 255–260. <https://doi.org/10.1002/ppp.618>
- Burd, K., Tank, S. E., Dion, N., Quinton, W. L., Spence, C., Tanentzap, A. J., & Olefeldt, D. (2018). Seasonal shifts in export of DOC and nutrients from burned and unburned peatland-rich catchments, Northwest Territories, Canada. *Hydrology and Earth System Sciences*, 22, 4455–4472. <https://doi.org/10.5194/hess-22-4455-2018>
- Burn, C. R. (1998). The response (1958–1997) of permafrost and near-surface ground temperatures to forest fire, Takhini River valley, southern Yukon Territory. *Canadian Journal of Earth Sciences*, 35(2), 184–199. <https://doi.org/10.1139/cj97-105>
- Camill, P. (1999). Peat accumulation and succession following permafrost thaw in the boreal peatlands of Manitoba, Canada. *Ecoscience*, 6(4), 592–602. <https://doi.org/10.1080/11956860.1999.11682561>
- Camill, P. (2005). Permafrost thaw accelerates in boreal peatlands during late-20th century climate warming. *Climatic Change*, 68(1–2), 135–152. <https://doi.org/10.1007/s10584-005-4785-y>
- Ciais, P., Sabine, C., Bala, G., Bopp, L., Brovkin, V., Canadell, J., et al. (2013). Carbon and other biogeochemical cycles. In T. F. Stocker (Eds.), *Climate change 2013: The physical science basis. Contribution of Working Group I to the Fifth Assessment Report of the Intergovernmental Panel on Climate Change* (pp. 465–570). Cambridge, UK, and New York, NY: Cambridge University Press.
- Cooper, M. D. A., Estop-Aragón, C., Fisher, J. P., Thierry, A., Garnett, M. H., Charman, D. J., et al. (2017). Limited contribution of permafrost carbon to methane release from thawing peatlands. *Nature Climate Change*, 7(7), 507–511. <https://doi.org/10.1038/NCLIMATE3328>
- Czimczik, C. I., Trumbore, S. E., Carbone, M. S., & Winston, G. C. (2006). Changing sources of soil respiration with time since fire in a boreal forest. *Global Change Biology*, 12(6), 957–971. <https://doi.org/10.1111/j.1365-2486.2006.01107.x>
- Czimczik, C. I., & Welker, J. M. (2010). Radiocarbon content of CO<sub>2</sub> respired from high Arctic tundra in Northwest Greenland. *Arctic, Antarctic, and Alpine Research*, 42(3), 342–350. <https://doi.org/10.1657/1938-4246-42.3.342>
- Dean, J. F., van der Velde, Y., Garnett, M. H., Dinsmore, K. J., Baxter, R., Lessels, J. S., et al. (2018). Abundant pre-industrial carbon detected in Canadian Arctic headwaters: Implications for the permafrost carbon feedback. *Environmental Research Letters*, 13(3), 034024. <https://doi.org/10.1088/1748-9326/aaa1fe>
- Dean, J. F., Garnett, M. H., Spyros, E., & Billett, M. F. (2019). The potential hidden age of dissolved organic carbon exported by peatland streams. *Journal of Geophysical Research: Biogeosciences*, 124, 328–341. <https://doi.org/10.1029/2018JG004650>
- Dean, J. F., Meisel, O. H., Martyn Rosco, M., Marchesini, L. B., Garnett, M. H., Lenderink, H., et al. (2020). East Siberian Arctic inland waters emit mostly contemporary carbon. *Nature Communications*, 11(1), 1–10. <https://doi.org/10.1038/s41467-020-15511-6>
- Drake, T. W., Guillemette, F., Hemingway, J. D., Chanton, J. P., Podgorski, D. C., Zimov, N. S., & Spencer, R. G. M. (2018). The ephemeral signature of permafrost carbon in an Arctic fluvial network. *Journal of Geophysical Research: Biogeosciences*, 123, 1475–1485. <https://doi.org/10.1029/2017JG004311>
- Drake, T. W., Wickland, K. P., Spencer, R. G. M., McKnight, D. M., & Striegl, R. G. (2015). Ancient low-molecular-weight organic acids in permafrost fuel rapid carbon dioxide production upon thaw. *Proceedings of the National Academy of Sciences*, 112(45), 13,946–13,951. <https://doi.org/10.1073/pnas.1511705112>
- Dutta, K., Schuur, E. A. G., Neff, J. C., & Zimov, S. A. (2006). Potential carbon release from permafrost soils of Northeastern Siberia. *Global Change Biology*, 12(12), 2336–2351. <https://doi.org/10.1111/j.1365-2486.2006.01259.x>
- Elder, C. D., Xu, X., Walker, J., Schnell, J. L., Hinkel, K. M., Townsend-Small, A., et al. (2018). Greenhouse gas emissions from diverse Arctic Alaskan lakes are dominated by young carbon. *Nature Climate Change*, 8(2), 166–171. <https://doi.org/10.1038/s41558-017-0066-9>

- Estop-Aragonés, C., Cooper, M. D. A., Fisher, J. P., Thierry, A., Garnett, M. H., Charman, D. J., et al. (2018). Limited release of previously-frozen C and increased new peat formation after thaw in permafrost peatlands. *Soil Biology and Biochemistry*, 118, 115–129. <https://doi.org/10.1016/j.soilbio.2017.12.010>
- Estop-Aragonés, C., Czimczik, C. I., Heffernan, L., Gibson, C., Walker, J. C., Xu, X., & Olefeldt, D. (2018). Respiration of aged soil carbon during fall in permafrost peatlands enhanced by active layer deepening following wildfire but limited following thermokarst. *Environmental Research Letters*, 13(8), 085002. <https://doi.org/10.1088/1748-9326/aad5f0>
- Ewing, S. A., O'Donnell, J. A., Aiken, G. R., Butler, K., Butman, D., Windham-Myers, L., & Kanevskiy, M. Z. (2015). Long-term anoxia and release of ancient, labile carbon upon thaw of Pleistocene permafrost. *Geophysical Research Letters*, 42, 10 730–10 738. <https://doi.org/10.1002/2015GL066296>
- Fellman, J. B., Hood, E., Raymond, P. A., Hudson, J., Bozeman, M., & Arimitsu, M. (2015). Evidence for the assimilation of ancient glacier organic carbon in a proglacial stream food web. *Limnology and Oceanography*, 60(4), 1118–1128. <https://doi.org/10.1002/lno.10088>
- Finlay, J., Neff, J., Zimov, S., Davydova, A., & Davydov, S. (2006). Snowmelt dominance of dissolved organic carbon in high-latitude watersheds: Implications for characterization and flux of river DOC. *Geophysical Research Letters*, 33, L10401. <https://doi.org/10.1029/2006GL025754>
- Fisher, J. P., Estop-Aragonés, C., Thierry, A., Charman, D. J., Wolfe, S. A., Hartley, I. P., et al. (2016). The influence of vegetation and soil characteristics on active-layer thickness of permafrost soils in boreal forest. *Global Change Biology*, 22(9), 3127–3140. <https://doi.org/10.1111/gcb.13248>
- Gandois, L., Hoyt, A. M., Hatté, C., Jeanneau, L., Teisserenc, R., Liotaud, M., & Tananaev, N. (2019). Contribution of peatland permafrost to dissolved organic matter along a thaw gradient in North Siberia. *Environmental Science and Technology*, 53(24), 14,165–14,174. <https://doi.org/10.1021/acs.est.9b03735>
- Gao, L., Zhou, Z., Reyes, A. V., & Guo, L. (2018). Yields and characterization of dissolved organic matter from different aged soils in northern Alaska. *Journal of Geophysical Research: Biogeosciences*, 123, 2035–2052. <https://doi.org/10.1029/2018JG004408>
- Gibson, C. M., Chasmer, L. E., Thompson, D. K., Quinton, W. L., Flannigan, M. D., & Olefeldt, D. (2018). Wildfire as a major driver of recent permafrost thaw in boreal peatlands. *Nature Communications*, 9(1), 3041. <https://doi.org/10.1038/s41467-018-05457-1>
- Godin, P. (2014). *Using lignin biomarkers and <sup>14</sup>C, of both river DOC and POC, and permafrost soils, to characterize the impacts of climate warming and permafrost degradation on the organic carbon budget of the Hudson Bay, Canada* (Master thesis) (pp. 1–103). Winnipeg, Manitoba, Canada: University of Manitoba. Retrieved from <https://mspace.lib.umanitoba.ca/xmlui/handle/1993/30177>
- Goni, M. A., Yunker, M. B., Macdonald, R. W., & Eglinton, T. I. (2005). The supply and preservation of ancient and modern components of organic carbon in the Canadian Beaufort Shelf of the Arctic Ocean. *Marine Chemistry*, 93(1), 53–73. <https://doi.org/10.1016/j.marchem.2004.08.001>
- Graven, H. D. (2015). Impact of fossil fuel emissions on atmospheric radiocarbon and various applications of radiocarbon over this century. *Proceedings of the National Academy of Sciences*, 112(31), 9542–9545. <https://doi.org/10.1073/pnas.1504467112>
- Grosse, G., Harden, J., Turetsky, M., McGuire, A. D., Camill, P., Tarnocai, C., et al. (2011). Vulnerability of high-latitude soil organic carbon in North America to disturbance. *Journal of Geophysical Research*, 116, G00K06. <https://doi.org/10.1029/2010JG001507>
- Grosse, G., Robinson, J., Bryant, R., Taylor, M. D., Harper, W., DeMasi, A., et al. (2013). *Distribution of late pleistocene ice-rich syngenetic permafrost of the Yedoma Suite in East and Central Siberia Russia* (Geological Survey open file report 2013-1078) (pp. 1–37). Reston, VA: U. S. Geological Survey.
- Guo, L., Lehner, J. K., White, D. M., & Garland, D. S. (2003). Heterogeneity of natural organic matter from the Chena River, Alaska. *Water Research*, 37(5), 1015–1022. [https://doi.org/10.1016/S0043-1354\(02\)00443-8](https://doi.org/10.1016/S0043-1354(02)00443-8)
- Guo, L., & Macdonald, R. W. (2006). Source and transport of terrigenous organic matter in the upper Yukon River: Evidence from isotope ( $\delta^{13}\text{C}$ ,  $\delta^{14}\text{C}$ , and  $\delta^{15}\text{N}$ ) composition of dissolved, colloidal, and particulate phases. *Global Biogeochemical Cycles*, 20, GB2011. <https://doi.org/10.1029/2005GB002593>
- Guo, L., Ping, C. L., & Macdonald, R. W. (2007). Mobilization pathways of organic carbon from permafrost to arctic rivers in a changing climate. *Geophysical Research Letters*, 34, L13603. <https://doi.org/10.1029/2007GL030689>
- Harden, J. W., Koven, C. D., Ping, C. L., Hugelius, G., David McGuire, A., Camill, P., et al. (2012). Field information links permafrost carbon to physical vulnerabilities of thawing. *Geophysical Research Letters*, 39, L15704. <https://doi.org/10.1029/2012GL051958>
- He, Y., Trumbore, S. E., Torn, M. S., Harden, J. W., Vaughn, L. J., Allison, S. D., & Randerson, J. T. (2016). Radiocarbon constraints imply reduced carbon uptake by soils during the 21st century. *Science*, 353(6306). <https://doi.org/10.1126/science.aad4273>
- Hicks Pries, C. E., Schuur, E. A. G., & Crummer, K. G. (2013). Thawing permafrost increases old soil and autotrophic respiration in tundra: Partitioning ecosystem respiration using  $^{13}\text{C}$  and  $^{14}\text{C}$ . *Global Change Biology*, 19(2), 649–661. <https://doi.org/10.1111/gcb.12058>
- Hicks Pries, C. E., Schuur, E. A. G., Natali, S. M., & Crummer, K. G. (2016). Old soil carbon losses increase with ecosystem respiration in experimentally thawed tundra. *Nature Climate Change*, 6(2), 214–218. <https://doi.org/10.1038/nclimate2830>
- Hicks Pries, C. E., Van Logtestijn, R. S. P., Schuur, E. A. G., Natali, S. M., Cornelissen, J. H. C., Aerts, R., & Dorrepaal, E. (2015). Decadal warming causes a consistent and persistent shift from heterotrophic to autotrophic respiration in contrasting permafrost ecosystems. *Global Change Biology*, 21(12), 4508–4519. <https://doi.org/10.1111/gcb.13032>
- Hilton, R. G., Galy, V., Gaillardet, J., Dellinger, M., Bryant, C., O'Regan, M., et al. (2015). Erosion of organic carbon in the Arctic as a geological carbon dioxide sink. *Nature*, 524(7563), 84–87. <https://doi.org/10.1038/nature14653>
- Holmes, R. M., McClelland, J. W., Tank, S. E., Spencer, R. G. M., & Shiklomanov, A. I. (2018). *Arctic Great Rivers Observatory (Water Quality Dataset)*. Falmouth, MA: Woodwell Climate Research Center. Retrieved from <http://www.Arcticgreatrivers.Org/Data>
- Holmes, R. M., McClelland, J. W., Raymond, P. A., Frazer, B. B., Peterson, B. J., & Stieglitz, M. (2008). Lability of DOC transported by Alaskan rivers to the Arctic Ocean. *Geophysical Research Letters*, 35, L03402. <https://doi.org/10.1029/2007GL032837>
- Holmes, R. M., McClelland, J. W., Peterson, B. J., Tank, S. E., Bulygina, E., Eglinton, T. I., et al. (2012). Seasonal and annual fluxes of nutrients and organic matter from large rivers to the Arctic Ocean and surrounding seas. *Estuaries and Coasts*, 35(2), 369–382. <https://doi.org/10.1007/s12237-011-9386-6>
- Hood, E., Fellman, J., Spencer, R. G. M., Hernes, P. J., Edwards, R., Damore, D., & Scott, D. (2009). Glaciers as a source of ancient and labile organic matter to the marine environment. *Nature*, 462(7276), 1044–1047. <https://doi.org/10.1038/nature08580>
- Hua, Q., Barbetti, M., & Rakowski, A. Z. (2013). Atmospheric radiocarbon for the period 1950–2010. *Radiocarbon*, 55(4), 2059–2072. [https://doi.org/10.2458/azu\\_js\\_rc.v55i2.16177](https://doi.org/10.2458/azu_js_rc.v55i2.16177)
- Huang, J., Zhang, X., Zhang, Q., Lin, Y., Hao, M., Luo, Y., et al. (2017). Recently amplified arctic warming has contributed to a continual global warming trend. *Nature Climate Change*, 7(12), 875–879. <https://doi.org/10.1038/s41558-017-0009-5>
- Jafarov, E. E., Coon, E. T., Harp, D. R., Wilson, C. J., Painter, S. L., Atchley, A. L., & Romanovsky, V. E. (2018). Modeling the role of preferential snow accumulation in through talik development and hillslope groundwater flow in a transitional permafrost landscape. *Environmental Research Letters*, 13(10), 105006. <https://doi.org/10.1088/1748-9326/aad3d0>



- Jansson, J. K., & Taş, N. (2014). The microbial ecology of permafrost. *Nature Reviews Microbiology*, 12(6), 414–425. <https://doi.org/10.1038/nrmicro3262>
- Jin, Q., & Bethke, C. M. (2005). Predicting the rate of microbial respiration in geochemical environments. *Geochimica et Cosmochimica Acta*, 69(5), 1133–1143. <https://doi.org/10.1016/j.gca.2004.08.010>
- Jorgenson, M. T., & Osterkamp, T. E. (2005). Response of boreal ecosystems to varying modes of permafrost degradation. *Canadian Journal of Forest Resources*, 35(9), 2100–2111. <https://doi.org/10.1139/X05-153>
- Kawahigashi, M., Kaiser, K., Kalbitz, K., Rodionov, A., & Guggenberger, G. (2004). Dissolved organic matter in small streams along a gradient from discontinuous to continuous permafrost. *Global Change Biology*, 10(9), 1576–1586. <https://doi.org/10.1111/j.1365-2486.2004.00827.x>
- Kawahigashi, M., Kaiser, K., Rodionov, A., & Guggenberger, G. (2006). Sorption of dissolved organic matter by mineral soils of the Siberian forest tundra. *Global Change Biology*, 12(10), 1868–1877. <https://doi.org/10.1111/j.1365-2486.2006.01203.x>
- Klapstein, S. J., Turetsky, M. R., McGuire, A. D., Harden, J. W., Czimczik, C. I., Xu, X., et al. (2014). Controls on methane released through ebullition in peatlands affected by permafrost degradation. *Journal of Geophysical Research: Biogeosciences*, 119, 418–431. <https://doi.org/10.1002/2013JG002441>
- Kokelj, S. V., Jenkins, R. E., Milburn, D., Burn, C. R., & Snow, N. (2005). The influence of thermokarst disturbance on the water quality of Small Upland Lakes, Mackenzie Delta Region, Northwest Territories, Canada. *Permafrost and Periglacial Processes*, 16, 343–353. <https://doi.org/10.1002/ppp.536>
- Kokelj, S. V., & Jorgenson, M. T. (2013). Advances in thermokarst research. *Permafrost and Periglacial Processes*, 24(2), 108–119. <https://doi.org/10.1002/ppp.1779>
- Kokelj, S. V., Lacelle, D., Lantz, T. C., Tunnicliffe, J., Malone, L., Clark, I. D., & Chin, K. S. (2013). Thawing of massive ground ice in mega slumps drives increases in stream sediment and solute flux across a range of watershed scales. *Journal of Geophysical Research: Earth Surface*, 118, 681–692. <https://doi.org/10.1002/jgrf.20063>
- Koven, C. D., Ringeval, B., Friedlingstein, P., Ciais, P., Cadule, P., Khvorostyanov, D., et al. (2011). Permafrost carbon-climate feedbacks accelerate global warming. *Proceedings of the National Academy of Sciences of the United States of America*, 108(36), 14,769–14,774. <https://doi.org/10.1073/pnas.1103910108>
- Lawrence, D. M., Koven, C. D., Swenson, S. C., Riley, W. J., & Slater, A. G. (2015). Permafrost thaw and resulting soil moisture changes regulate projected high-latitude CO<sub>2</sub> and CH<sub>4</sub> emissions. *Environmental Research Letters*, 10(9), 094011. <https://doi.org/10.1088/1748-9326/10/9/094011>
- Lee, H., Schuur, E. A. G., Inglett, K. S., Lavoie, M., & Chanton, J. P. (2012). The rate of permafrost carbon release under aerobic and anaerobic conditions and its potential effects on climate. *Global Change Biology*, 18(2), 515–527. <https://doi.org/10.1111/j.1365-2486.2011.02519.x>
- Letscher, R. T., Hansell, D. A., & Kadko, D. (2011). Rapid removal of terrigenous dissolved organic carbon over the Eurasian shelves of the Arctic Ocean. *Marine Chemistry*, 123(1–4), 78–87. <https://doi.org/10.1016/j.marchem.2010.10.002>
- Littlefair, C. A., Tank, S. E., & Kokelj, S. V. (2017). Retrogressive thaw slumps temper dissolved organic carbon delivery to streams of the Peel Plateau, NWT, Canada. *Biogeosciences*, 14(23), 5487–5505. <https://doi.org/10.5194/bg-14-5487-2017>
- Lupascu, M., Czimczik, C. I., Welker, M. C., Ziolkowski, L. A., Cooper, E. J., & Welker, J. M. (2018). Winter ecosystem respiration and sources of CO<sub>2</sub> from the High Arctic Tundra of Svalbard: Response to a deeper snow experiment. *Journal of Geophysical Research: Biogeosciences*, 123, 2627–2642. <https://doi.org/10.1029/2018JG004396>
- Lupascu, M., Welker, J. M., Seibt, U., Maseyk, K., Xu, X., & Czimczik, C. I. (2014). High Arctic wetting reduces permafrost carbon feedbacks to climate warming. *Nature Climate Change*, 4(1), 51–55. <https://doi.org/10.1038/nclimate2058>
- Lupascu, M., Welker, J. M., Xu, X., & Czimczik, C. I. (2014). Rates and radiocarbon content of summer ecosystem respiration in response to long-term deeper snow in the High Arctic of NW Greenland. *Journal of Geophysical Research: Biogeosciences*, 119, 1180–1194. <https://doi.org/10.1002/2013JG002494>
- Mackelprang, R., Saleska, S. R., Jacobsen, C. S., Jansson, J. K., & Taş, N. (2016). Permafrost meta-omics and climate change. *Annual Review of Earth and Planetary Sciences*, 44(1), 439–462. <https://doi.org/10.1146/annurev-earth-060614-105126>
- Mann, P. J., Eglinton, T. I., McIntyre, C. P., Zimov, N., Davydova, A., Vonk, J. E., et al. (2015). Utilization of ancient permafrost carbon in headwaters of Arctic fluvial networks. *Nature Communications*, 6, 1–7. <https://doi.org/10.1038/ncomms8856>
- Martens, C. S., Kelley, C. A., Chanton, J. P., & Showers, W. J. (1992). Carbon and hydrogen isotopic characterization of methane from wetlands and lakes of the Yukon-Kuskokwim Delta, Western Alaska. *Journal of Geophysical Research*, 97(D15), 16,689–16,701. <https://doi.org/10.1029/91JD02885>
- McCallister, S. L., & del Giorgio, P. A. (2012). Evidence for the respiration of ancient terrestrial organic C in northern temperate lakes and streams. *Proceedings of the National Academy of Sciences*, 109(42), 16,963–16,968. <https://doi.org/10.1073/pnas.1207305109>
- McClelland, J. W., Holmes, R. M., Peterson, B. J., Raymond, P. A., Striegl, R. G., Zhulidov, A. V., et al. (2016). Particulate organic carbon and nitrogen export from major Arctic rivers. *Global Biogeochemical Cycles*, 30, 1–15. <https://doi.org/10.1002/2015GB005351>
- Metcalfe, D. B., Hermans, T. D. G., Ahlstrand, J., Becker, M., Berggren, M., Björk, R. G., et al. (2018). Patchy field sampling biases understanding of climate change impacts across the Arctic. *Nature Ecology and Evolution*, 2, 1443–1448. <https://doi.org/10.1038/s41559-018-0612-5>
- Moore, J. W., & Semmens, B. X. (2008). Incorporating uncertainty and prior information into stable isotope mixing models. *Ecology Letters*, 11(5), 470–480. <https://doi.org/10.1111/j.1461-0248.2008.01163.x>
- Nakagawa, F., Yoshida, N., Nojiri, Y., & Makarov, V. (2002). Production of methane from alases in eastern Siberia: Implications from its 14 C and stable isotopic compositions. *Global Biogeochemical Cycles*, 16(3), <https://doi.org/10.1029/2000GB001384>
- Natali, S. M., Schuur, E. A. G., Mauritz, M., Schade, J. D., Celis, G., Crummer, K. G., et al. (2015). Permafrost thaw and soil moisture driving CO<sub>2</sub> and CH<sub>4</sub> release from upland tundra. *Journal of Geophysical Research: Biogeosciences*, 120, 525–537. <https://doi.org/10.1002/2014JG002872>
- Natali, S. M., Schuur, E. A. G., Trucco, C., Hicks Pries, C. E., Crummer, K. G., & Baron Lopez, A. F. (2011). Effects of experimental warming of air, soil and permafrost on carbon balance in Alaskan tundra. *Global Change Biology*, 17(3), 1394–1407. <https://doi.org/10.1111/j.1365-2486.2010.02303.x>
- Neff, J. C., Finlay, J. C., Zimov, S. A., Davydov, S. P., Carrasco, J. J., Schuur, E. A. G., & Davydova, A. I. (2006). Seasonal changes in the age and structure of dissolved organic carbon in Siberian rivers and streams. *Geophysical Research Letters*, 33, L23401. <https://doi.org/10.1029/2006GL028222>



- Negandhi, K., Laurion, I., Whitticar, M. J., Galand, P. E., Xu, X., & Lovejoy, C. (2013). Small thaw ponds: An unaccounted source of methane in the Canadian high Arctic. *PLoS ONE*, 8(11). <https://doi.org/10.1371/journal.pone.0078204>
- Nitze, I., Grosse, G., Jones, B. M., Romanovsky, V. E., & Boike, J. (2018). Remote sensing quantifies widespread abundance of permafrost region disturbances across the Arctic and Subarctic. *Nature Communications*, 9(1), 5423. <https://doi.org/10.1038/s41467-018-07663-3>
- Nowinski, N. S., Taneva, L., Trumbore, S. E., & Welker, J. M. (2010). Decomposition of old organic matter as a result of deeper active layers in a snow depth manipulation experiment. *Oecologia*, 163(3), 785–792. <https://doi.org/10.1007/s00442-009-1556-x>
- O'Donnell, J. A., Aiken, G. R., Butler, K. D., Guillemette, F., Podgorski, D. C., & Spencer, R. G. M. (2016). DOM composition and transformation in boreal forest soils: The effects of temperature and organic-horizon decomposition state. *Journal of Geophysical Research: Biogeosciences*, 121, 2727–2744. <https://doi.org/10.1002/2016JG003431>. Received
- O'Donnell, J. A., Aiken, G. R., Walvoord, M. A., Raymond, P. A., Butler, K. D., Domblaser, M. K., & Heckman, K. (2014). Using dissolved organic matter age and composition to detect permafrost thaw in boreal watersheds of interior Alaska. *Journal of Geophysical Research: Biogeosciences*, 119, 2155–2170. <https://doi.org/10.1002/2014JG002695>
- O'Donnell, J. A., Aiken, G. R., Walvoord, M. A., & Butler, K. D. (2012). Dissolved organic matter composition of winter flow in the Yukon River basin: Implications of permafrost thaw and increased groundwater discharge. *Global Biogeochemical Cycles*, 26, GB0E06. <https://doi.org/10.1029/2012GB004341>
- O'Donnell, J. A., Harden, J. W., McGuire, A. D., Kanevskiy, M. Z., Jorgenson, M. T., & Xu, X. (2011). The effect of fire and permafrost interactions on soil carbon accumulation in an upland black spruce ecosystem of interior Alaska: Implications for post-thaw carbon loss. *Global Change Biology*, 17(3), 1461–1474. <https://doi.org/10.1111/j.1365-2486.2010.02358.x>
- Olefeldt, D., Goswami, S., Grosse, G., Hayes, D., Hugelius, G., Kuhry, P., et al. (2016). Circumpolar distribution and carbon storage of thermokarst landscapes. *Nature Communications*, 7(1), 1–11. <https://doi.org/10.1038/ncomms13043>
- Pack, M. A., Xu, X., Lupascu, M., Kessler, J. D., & Czimeczik, C. I. (2015). A rapid method for preparing low volume CH<sub>4</sub> and CO<sub>2</sub> gas samples for 14C AMS analysis. *Organic Geochemistry*, 78, 89–98. <https://doi.org/10.1016/j.orggeochem.2014.10.010>
- Philippson, B. (2013). The freshwater reservoir effect in radiocarbon dating. *Heritage Science*, 1(1), 24–19. <https://doi.org/10.1186/2050-7445-1-24>
- Raymond, P. A., McClelland, J. W., Holmes, R. M., Zhulidov, A. V., Mull, K., Peterson, B. J., et al. (2007). Flux and age of dissolved organic carbon exported to the Arctic Ocean: A carbon isotopic study of the five largest arctic rivers. *Global Biogeochemical Cycles*, 21, GB4011. <https://doi.org/10.1029/2007GB002934>
- Raymond, P. A., Saiers, J. E., & Sobczak, W. V. (2016). Hydrological and biogeochemical controls on watershed DOM transport: Pulse-shunt concept. *Ecology*, 97(1), 5–16. <https://doi.org/10.1890/14-1684.1>
- Regnier, P., Friedlingstein, P., Ciais, P., Mackenzie, F. T., Gruber, N., Janssens, I. A., et al. (2013). Anthropogenic perturbation of the carbon fluxes from land to ocean. *Nature Geoscience*, 6(8), 597–607. <https://doi.org/10.1038/ngeo1830>
- Schädel, C., Bader, M. K.-F., Schuur, E. A. G., Biasi, C., Bracho, R., Čapek, P., et al. (2016). Potential carbon emissions dominated by carbon dioxide from thawed permafrost soils. *Nature Climate Change*, 6(10), 950–953. <https://doi.org/10.1038/nclimate3054>
- Schaefer, K., Lantuit, H., Romanovsky, V. E., Schuur, E. A. & Witt, R. (2014). The impact of the permafrost carbon feedback on global climate. *Environmental Research Letters*, 9(8), 085003. <https://doi.org/10.1088/1748-9326/9/8/085003>
- Schirrmeister, L., Froese, D., Tumskey, V., Grosse, G., & Wetterich, S. (2013). Yedoma: Late Pleistocene ice-rich syngenetic permafrost of Beringia. In S. A. Elias (Ed.), *Encyclopedia of quaternary science* (Vol. 3, 2nd ed., pp. 542–552). Amsterdam: Elsevier.
- Schuur, E. A. G., McGuire, A. D., Grosse, G., Harden, J. W., Hayes, D. J., Hugelius, G., et al. (2015). Climate change and the permafrost carbon feedback. *Nature*, 520, 171–179. <https://doi.org/10.1038/nature14338>
- Schuur, E. A. G., Druffel, E. R., & Trumbore, S. E. (2016). Radiocarbon and climate change: Mechanisms, applications and laboratory techniques. In *Radiocarbon and climate change* (pp. 45–82). Switzerland: Springer International Publishing.
- Schuur, E. A. G., McGuire, A. D., Romanovsky, V., Schädel, C., & Mack, M. (2018). Arctic and boreal carbon. In N. Cavallaro, et al (Eds.), *Second State of the Carbon Cycle Report (SOCCR2): A sustained assessment report* (pp. 428–468). Washington, DC, USA: U.S. Global Change Research Program.
- Schuur, E. A. G., & Trumbore, S. E. (2006). Partitioning sources of soil respiration in boreal black spruce forest using radiocarbon. *Global Change Biology*, 12(2), 165–176. <https://doi.org/10.1111/j.1365-2486.2005.01066.x>
- Schuur, E. A. G., Vogel, J. G., Crummer, K. G., Lee, H., Sickman, J. O., & Osterkamp, T. E. (2009). The effect of permafrost thaw on old carbon release and net carbon exchange from tundra. *Nature*, 459(7246), 556–559. <https://doi.org/10.1038/nature08031>
- Spencer, R. G. M., Mann, P. J., Dittmar, T., Eglinton, T. I., McIntyre, C., Holmes, R. M., et al. (2015). Detecting the signature of permafrost thaw in Arctic rivers. *Geophysical Research Letters*, 42, 2830–2835. <https://doi.org/10.1002/2015GL063498>
- Strauss, J., Schirrmeister, L., Grosse, G., Fortier, D., Hugelius, G., Knoblauch, C., et al. (2017). Deep Yedoma permafrost: A synthesis of depositional characteristics and carbon vulnerability. *Earth-Science Reviews*, 172, 75–86. <https://doi.org/10.1016/j.earscirev.2017.07.007>
- Striegl, R. G., Domblaser, M. M., Aiken, G. R., Wickland, K. P., & Raymond, P. A. (2007). Carbon export and cycling by the Yukon, Tanana, and Porcupine rivers, Alaska, 2001–2005. *Water Resources Research*, 43, W02411. <https://doi.org/10.1029/2006WR005201>
- Stubbins, A., Hood, E., Raymond, P. A., Aiken, G. R., Sleighter, R. L., Hernes, P. J., et al. (2012). Anthropogenic aerosols as a source of ancient dissolved organic matter in glaciers. *Nature Geoscience*, 5(3), 198–201. <https://doi.org/10.1038/ngeo1403>
- Stuiver, M., & Polach, H. A. (1977). Discussion: Reporting of 14 C data. *Radiocarbon*, 19(3), 355–363. <https://doi.org/10.1021/ac100494m>
- Tank, S. E., Fellman, J. B., Hood, E., & Krutzberg, E. S. (2018). Beyond respiration: Controls on lateral carbon fluxes across the terrestrial-aquatic interface. *Limnology and Oceanography Letters*, 76–88. <https://doi.org/10.1002/lol2.10065>
- Toohy, R. C., Herman-Mercer, N. M., Schuster, P. F., Mutter, E. A., & Koch, J. C. (2016). Multidecadal increases in the Yukon River Basin of chemical fluxes as indicators of changing flowpaths, groundwater, and permafrost. *Geophysical Research Letters*, 43, 12,120–12,130. <https://doi.org/10.1002/2016GL070817>
- Treat, C. C., Natali, S. M., Ernakovich, J., Iversen, C. M., Lupascu, M., McGuire, A. D., et al. (2015). A pan-Arctic synthesis of CH<sub>4</sub> and CO<sub>2</sub> production from anoxic soil incubations. *Global Change Biology*, 21(7), 2787–2803. <https://doi.org/10.1111/gcb.12875>
- Trumbore, S. (2000). Age of soil organic matter and soil respiration: Radiocarbon constraints on belowground C dynamics. *Ecological Applications*, 10(2), 399–411. [https://doi.org/10.1890/1051-0761\(2000\)010\[0399:AOSOMA\]2.0.CO;2](https://doi.org/10.1890/1051-0761(2000)010[0399:AOSOMA]2.0.CO;2)
- Trumbore, S. (2009). Radiocarbon and soil carbon dynamics. *Annual Review of Earth and Planetary Sciences*, 37(1), 47–66. <https://doi.org/10.1146/annurev.earth.36.031207.124300>
- Turetsky, M. R., Wieder, R. K., Williams, C. J., & Vitt, D. H. (2000). Organic matter accumulation, peat chemistry, and permafrost melting in peatlands of boreal Alberta. *Ecoscience*, 7(3), 379–392. <https://doi.org/10.1080/11956860.2000.11682608>
- Vonk, J. E., Tank, S. E., Bowden, W. B., Laurion, I., Vincent, W. F., Alekseychik, P., et al. (2015). Reviews and syntheses: Effects of permafrost thaw on Arctic aquatic. *Biogeosciences*, 12, 7129–7167. <https://doi.org/10.5194/bg-12-7129-2015>

- Vonk, J. E., Tank, S. E., Mann, P. J., Spencer, R. G. M., Treat, C. C., Striegl, R. G., et al. (2015). Biodegradability of dissolved organic carbon in permafrost soils and aquatic systems: A meta-analysis. *Biogeosciences*, 12(23), 6915–6930. <https://doi.org/10.5194/bg-12-6915-2015>
- Vonk, J. E., Mann, P. J., Davydov, S., Davydova, A., Spencer, R. G. M., Schade, J., et al. (2013). High biolability of ancient permafrost carbon upon thaw. *Geophysical Research Letters*, 40, 2689–2693. <https://doi.org/10.1002/grl.50348>
- Walter Anthony, K., Daanen, R., Anthony, P., Schneider Von Deimling, T., Ping, C. L., Chanton, J. P., & Grosse, G. (2016). Methane emissions proportional to permafrost carbon thawed in Arctic lakes since the 1950s. *Nature Geoscience*, 9(9), 679–682. <https://doi.org/10.1038/ngeo2795>
- Walter Anthony, K., Schneider von Deimling, T., Nitze, I., Frolking, S., Emond, A., Daanen, R., et al. (2018). 21st-century modeled permafrost carbon emissions accelerated by abrupt thaw beneath lakes. *Nature Communications*, 9(1), 3262. <https://doi.org/10.1038/s41467-018-05738-9>
- Walter, K. M., Chanton, J. P., Chapin, F. S., Schuur, E. A. G., & Zimov, S. A. (2008). Methane production and bubble emissions from arctic lakes: Isotopic implications for source pathways and ages. *Journal of Geophysical Research: Biogeosciences*, 113, G00A08. <https://doi.org/10.1029/2007JG000569>
- Wild, B., Andersson, A., Bröder, L., Vonk, J., Hugelius, G., McClelland, J. W., et al. (2019). Rivers across the Siberian Arctic unearth the patterns of carbon release from thawing permafrost. *Proceedings of the National Academy of Sciences of the United States of America*, 116(21), 10,280–10,285. <https://doi.org/10.1073/pnas.1811797116>
- Wilson, R. M., Fitzhugh, L., Whiting, G. J., Frolking, S., Harrison, M. D., Dimova, N., et al. (2017). Greenhouse gas balance over thaw-freeze cycles in discontinuous zone permafrost. *Journal of Geophysical Research: Biogeosciences*, 122, 387–404. <https://doi.org/10.1002/2016JG003600>
- Xu, C., Guo, L., Dou, F., & Ping, C. L. (2009). Potential DOC production from size-fractionated Arctic tundra soils. *Cold Regions Science and Technology*, 55(1), 141–150. <https://doi.org/10.1016/j.coldregions.2008.08.001>
- Zimov, S. A., Voropaev, Y. V., Semiletov, I. P., Davidov, S. P., Prosiannikov, S. F., Chapin, F. S. III, et al. (1997). North Siberian lakes: A methane source fueled by Pleistocene carbon. *Science*, 277(5327), 800–802. <https://doi.org/10.1126/science.277.5327.800>